JOURNAL OF THE AERONAUTICAL SCIENCES

VOLUME 8 FEBRUARY, 1941 NUMBER 4

Airplane Performance Testing at Altitude

ALBERT C. REED

Boeing Aircraft Company

Introduction

The flight testing of airplanes in the past frequently has lent itself to methods of procedure somewhat less scientific than adventurous. It has always been a job fraught with uncertainties: the uncertainties of the weather, uncertainties of instruments and their functioning in flight conditions, uncertainties of scientific observation under conditions of discomfort and distraction, and uncertainties of the full meaning of the measurements made. The records obtained in flight have often been so inaccurate that no reliance could be placed upon them. The airplane may not have been flown steadily or long enough under steady conditions to establish a stabilized state of motion. The power of the engine has been indeterminate depending upon a great many variables, few of which, as a rule, have been measurable. The atmosphere is a fluid of uncertain motion and density. Drag items on the airplane, variables in themselves, are frequently not under control. Finally, the technique of flight testing is still not very fully developed.

Attempts made to compare the performance of two or more airplanes frequently lead to the conclusion that when the airplanes are not tested on the same type of day, with similar temperature conditions, the results are not comparable. Full-throttle ceiling may vary as much as fifteen per cent from day to day, and methods of reducing it to "standard conditions" are controversial. Level speeds have been so inaccurately measured and reduced to standard that the results of such testing at one time became usable only as very questionable sales figures. As a matter of fact, the airplane manufacturer himself frequently had no more than a vague idea of the real basic performance of his aircraft.

Presented at the I.Ae.S. session of the A.A.A.S. Meeting, University of Washington, Seattle, June 21, 1940.

Historical Sketch of Flight Testing

One of the first attempts to reduce this flight test uncertainty was made by the British National Physical Laboratory. Early in the last war Tizard and Bairstow developed the method used at the Experimental Aircraft Testing Station in England. There pilots were trained in technique and engineers were trained in methods of handling the flight data. At the same time flight test procedures were developed independently in France, and in 1918 there was a hot controversy over the superiority of the English *vs.* the French methods.

In the United States two schools of thought developed. The Army airplane testing activities early concentrated at Dayton, Ohio, where a group of test pilots and test engineers developed the Army method of flight testing and manipulation of the flight test data to give results obtainable under ideal standard conditions. This technique has been called the Army method of reduction. The Navy, starting from a somewhat theoretical standpoint, developed both flight testing technique and reduction methods on a different basis. This method has variously been called the Navy method or the Diehl method.* Efforts made to coordinate the Army and Navy methods were never very successful.

All attempts to obtain greater precision in measuring aircraft performance gain their impetus largely from the still disconcerting discrepancy between flight test results obtained by different pilots flying in different atmospheric conditions and reducing their data in different ways. Explanations for these differences and theories, to bring them into conformity, have been elaborate. Frequently the method used was to take a quantity of empirical flight data and from the percentage variation determine constants which would reduce the discrepancy.

Recent developments of the theoretical knowledge of

* *Engineering Aerodynamics* by Walter Stewart Diehl; The Ronald Press Company, New York, 1936.

airplane performance variation with the factors influencing it have now provided a tool which, together with improved technique in obtaining accurate flight data, makes the measurement of airplane performance as accurate as other similar engineering measurements. The fact that it is not possible to climb as high with a given airplane on a hot summer day as on a cold winter day does not alter the basic performance of the airplane.

The Generalized Conception of Airplane Performance Testing

Airplane velocity and climb-rate are the results of work done by the engine through the medium of the propeller. Since the level speed of the airplane is merely the condition of zero climb for any given operating condition defined by the weight, power, propeller r.p.m., and density altitude, the performance of the airplane for this operating condition can be expressed by a curve of climb-rate *vs.* velocity. Fig. 1 illustrates such a curve of climb-rate *vs.* velocity (C_h *vs.* V) for constant

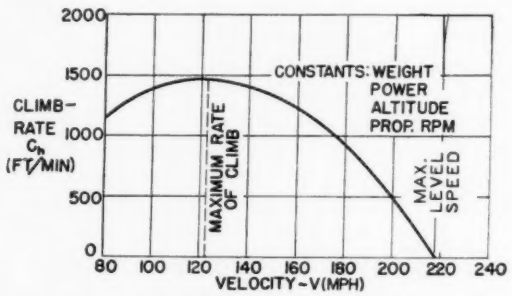

Fig. 1. Climb and high speed performance.

values of weight (W), power (P), propeller r.p.m. (N), and atmospheric density ratio (σ). A series of C_h *vs.* V curves may be constructed to express completely the performance of the airplane for all possible operating conditions, each of which would be defined by a different set of the variables W, P, N, and σ.

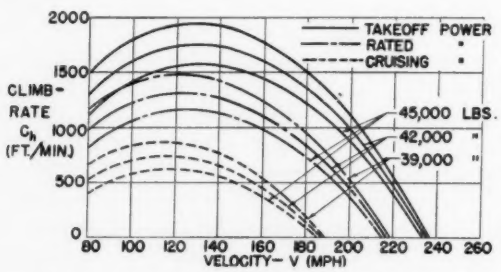

Fig. 2. Effect of weight and power on the performance at sea level.

The effect of weight and power on the performance of a typical airplane is illustrated in Fig. 2. The performance was computed for three combinations of weight and power for constant sea level density altitudes and constant propeller r.p.m. for each power condition (but differing from one power to another).

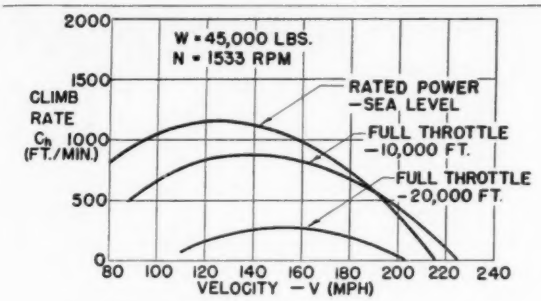

Fig. 3. Effect of altitude on performance.

The effect of altitude (at standard conditions) is shown in Fig. 3 for the constant values of weight and propeller r.p.m., as given with the figure.

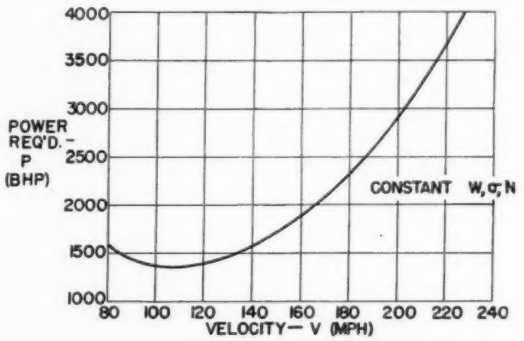

Fig. 4. Power required for level flight.

The points of zero climb-rate for the various operating conditions, as in Fig. 2, represent the respective velocities in level flight. These points may be plotted on a chart of power *vs.* velocity for constant W, σ, and N. Expressed in these terms the curve represents the fundamental of airplane performance. The curve of Fig. 4 shows the relationship of power and velocity in level flight for constant weight, W, constant relative density, σ, and constant propeller r.p.m., N. In order

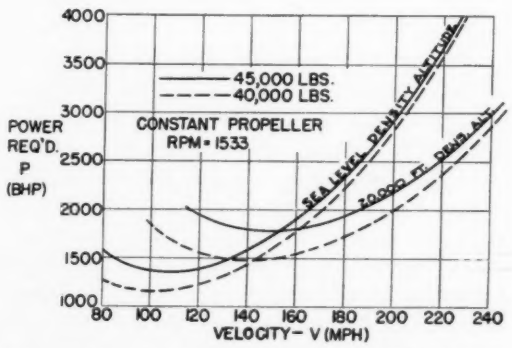

Fig. 5. Effect of weight and density altitude on power required for level flight.

to show the effects of the variables, weight and density, upon the power required to produce a certain velocity, Fig. 4 has been replotted for a typical airplane in Fig. 5. Two weights and two typical altitudes are shown.

The effect of the variable N is shown in Fig. 6. This effect can be seen to be relatively minor and is due primarily to small changes in propeller efficiency. For the full range of densities and weights, a great many of these charts would be necessary were it not for the fact that the effect of weight and density can be eliminated by changing the factors power, velocity, r.p.m., and climb-rate, to parameters involving weight and density.

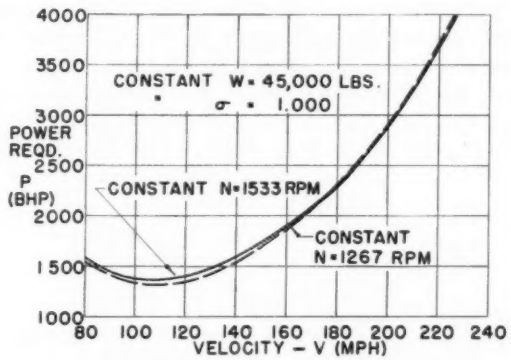

FIG. 6. Effect of propeller r.p.m. on the power required for level flight.

The first two of these parameters are P_{iw} and V_{iw}, respectively, and are defined as follows:

$$P_{iw} = \frac{\sigma^{1/2}P}{\left(\frac{W}{W_s}\right)^{3/2}} \text{ and } V_{iw} = \frac{\sigma^{1/2}V}{\left(\frac{W}{W_s}\right)^{1/2}}$$

where W = weight for which additional performance may be desired.

W_s = A standard reference gross weight for which the power-required curve is determined for sea level density altitude.

P = Brake power available.

V = True velocity (true air speed).

The fundamental performance curve, as given in Fig. 4, depends upon the three variables, W, σ, and N. Changing the coordinates to P_{iw} and V_{iw}, in accordance with the above equations, eliminates the variables W and σ, and thereby effects a general applicability of the curve to all altitudes and all weights. The variable N must also be written in terms of W and σ. This introduces a third parameter, N_{iw}, defined by the relation $\sigma^{1/2}N/\left(\frac{W}{W_s}\right)^{1/2}$. Fig. 7 may therefore be drawn, as in Fig. 4, to present a generalized power-required curve for a constant value of N_{iw}. Variations of N_{iw} correspond exactly to variations in N of Fig. 6.

The generalization effected by the introduction of the basic parameters involving density and weight can be

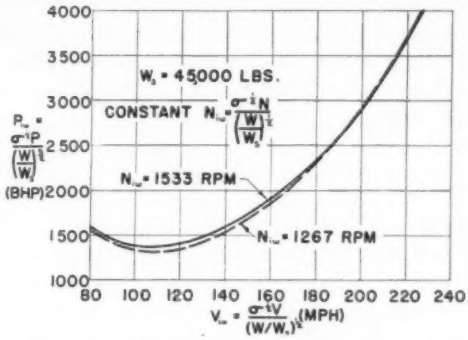

FIG. 7. Power required in level flight at constant N_{iw} for any weight and altitude.

used also with the climb-rate relationship of Fig. 3. The climb-rate parameter involving these variables is termed C_{iw} and it is similarly formed by multiplying climb-rate by the square root of the density ratio and dividing by the square root of the weight ratio; that is, $C_{iw} = \sigma^{1/2}C_k/\left(\frac{W}{W_s}\right)^{1/2}$. Curves of climb-rate plotted in this manner are for constant values of P_{iw} and N_{iw}. Fig. 3 is replotted in Fig. 8 for constant values of P_{iw} and N_{iw}. If the range of these curves is great enough, the complete plot will represent the total performance of the airplane.*

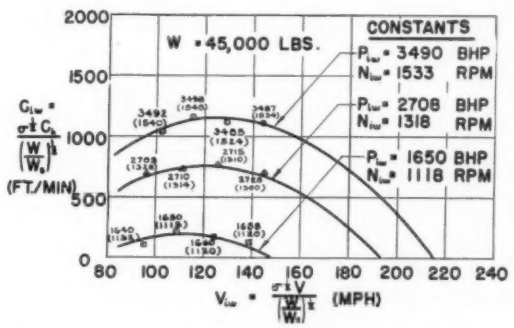

FIG. 8. Climb performance for any weight and altitude at constant P_{iw} and N_{iw}.

A further approach to fundamentals in determining airplane performance is possible by reducing weight to lift coefficient and reducing power required to drag coefficient. This is illustrated in Fig. 9. This familiar form of the performance curve is frequently referred to as the airplane's "polar."

While this curve is not a true parabola, the part of the curve covering the operating range of the airplane so

* The performance parameters appear simply and logically in the fundamental airplane performance equation for steady straight flight. (See N.A.C.A. Technical Report No. 408, *General Formulas and Charts for the Calculation of Airplane Performance* by W. Bailey Oswald, 1932. See also *Applied Aerodynamics* by Leonard Bairstow; Longmans, Green and Co., New York, 1939.

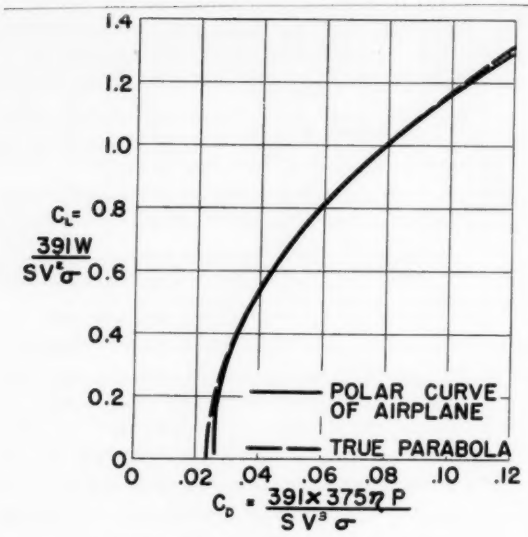

FIG. 9. Polar curve of typical airplane.

closely approximates a parabola that, for simplicity, the most useful part of the curve can be plotted as a straight line with the coordinates C_L^2 and C_D, as in Fig. 10.

The "polar" of an airplane is not constant for the various conditions of power. Increase in power in general increases the drag of the portion of the airplane in the slipstream because of the increased air velocity.

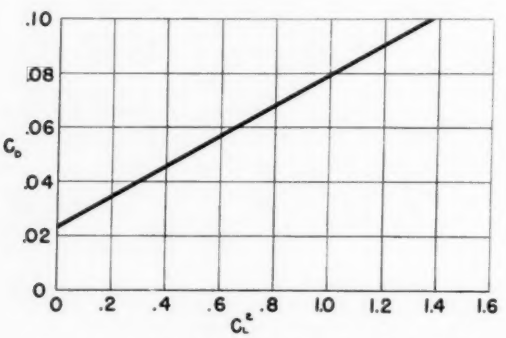

FIG. 10. Straight line assumption of polar curve.

The lift distribution is affected by the slipstream passing over portions of the wing. Change in the lift distribution in general changes the induced drag. The propeller thrust in general has a lift component. The lift distribution and the lift component of the thrust affect the angle of attack necessary for a given lift coefficient. The turbulence and pulsating nature of the slipstream affect both the lift and drag. All of these power factors affect the polar. However, the first, the increase in drag directly due to increased air velocity in the slipstream, is normally taken into account in the propeller efficiency. Such method is an approximation at the best, but it is a simple one. If the profile drag coefficient of the portion of the airplane included in the slipstream is essentially constant, the slipstream velocity effect may be expressed as a constant factor of propeller efficiency. Cowl flaps and other variables complicate or invalidate this method. However, the use of this method defines propulsive efficiency, which is propeller efficiency reduced to account for the increase in drag directly due to increase in velocity in the slipstream. It may be defined as the overall efficiency of the propeller in developing thrust with respect to the entire airplane. Precisely this is not true because of the other effects ot the slipstream on the polar. When analyzing flight test data, these other effects are more simply represented as changes in the polar than as changes in propeller efficiency. Thus, a family of polars can be drawn for various power conditions, as in Fig. 11.

Each polar of Fig. 11 is assumed to be for constant

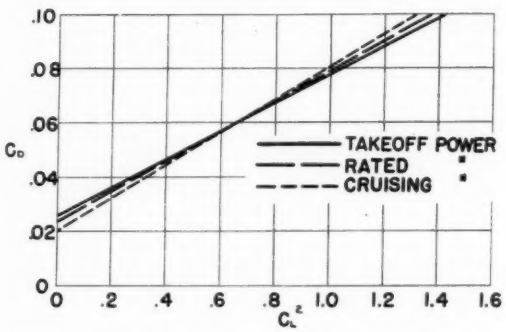

FIG. 11. Effect of power on lift and drag characteristics.

power parameter (P_{iw}). They could equally well be drawn for constant values of the climb-rate parameter (C_{iw}). Variations of the r.p.m. parameter N_{iw} introduce a family of curves for each of these conditions.

THE CONCEPTION OF STANDARD ALTITUDE

Standard altitude is defined by a sea level temperature and pressure and a vertical temperature gradient. These are empirical figures supposed to represent a mean for temperate zone latitudes. These three quantities determine a definite relation between temperature, pressure, density, and altitude. This relationship is illustrated in Fig. 12. For every pressure there is defined an altitude, and a scale of these altitudes can be used to calibrate a barometer. Then in the standard atmosphere this calibrated barometer may be used to measure altitude. In atmospheric conditions that are not standard, such a barometer offers an approximate measure of altitude. Altitude determined on this basis is called pressure altitude.

Corresponding to this pressure scale there is also a density scale of altitude. If a density-measuring instrument were available, it could be calibrated to

measure altitude accurately in a standard atmosphere. As in the case of the barometer, this might be used even in a non-standard atmosphere as an approximation. Altitudes measured on this scale are density altitudes.

Every combination of pressure and temperature in the atmosphere defines a density and therefore a density altitude. This suggests the plotting of a chart from

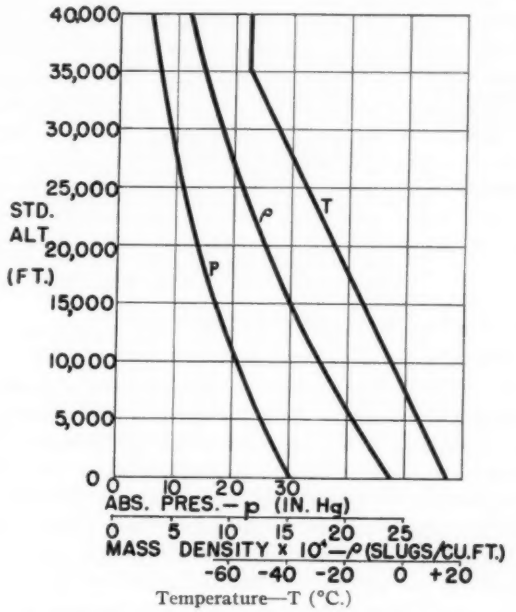

FIG. 12. Standard altitude characteristics.

which density altitude can be read directly for any combination of pressure and temperature. Such a chart is illustrated in Fig. 13.

THE REDUCTION OF FLIGHT TEST DATA

A. *Airspeed Calibration.* The actual performance of the airplane may be measured in flight test, but this performance applies only to the conditions under which the test may be performed. The problem of reducing the flight test data is that of reducing the data to given conditions of weight, density, power, r.p.m., mixture, and any of the other several factors affecting performance.

It is necessary to correct for weight, because it is impossible to perform any flight tests at constant weight, except performance in a truly power-off condition. The operation of the engines continuously consumes fuel and thereby reduces the weight. The variation in temperature and pressure relation in the atmosphere from day to day, and even hour to hour or minute to minute, makes it impossible to complete any flight test under fixed temperature and pressure relations in the atmosphere. In other words, flight test performance data must be corrected for temperature and density. The power and r.p.m., of course, may be controlled within limits during the flight test; however, all of the possible conditions of power and r.p.m. cannot be covered in any conceivably reasonable period of flight test time. This makes it necessary to interpolate flight test data and in some cases extrapolate the data for the desired conditions of power and r.p.m. Correction for engine operating mixture is also necessary.

First of all, the instrument installation for measuring the air speed must be calibrated and corrected for the variables affecting it. The first of these variables is the weight. The angle of attack of the airplane for given indicated air speed, power, r.p.m., lift,* and drag* conditions is a function of weight. The greater the weight, the greater the angle of attack, and *vice versa.*

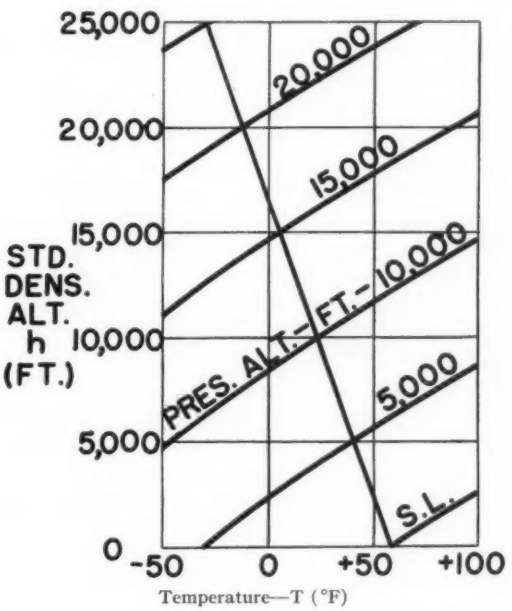

FIG. 13. Density altitude in terms of pressure altitude and temperature.

The error introduced by the pitot installation normally may be considered purely a function of angle of attack. Of course it is conceivable that a pitot location might be such that other factors might also introduce appreciable errors. The usual location of the pitot in the vicinity of the leading edge of the wing toward the wing tip or the vicinity of the nose of the fuselage or hull is essentially free from these other errors. It is therefore clear that an accurate air speed installation calibration would be in the form of a plot of percentage error against angle of attack. Neglecting certain factors, the angle of attack is a function of the lift coefficient. In level flight the lift coefficient is equal to the weight of the airplane divided by the dynamic pressure and the wing area,

* Lift and drag conditions may be varied by wing flaps, etc.

$C_L = \frac{W}{qS} = \frac{W}{\rho_{0/2}\sigma V^2 S}$.† Of the dynamic pressure the factor of one-half the standard sea level density is constant and for any given airplane the wing area is constant, at least for present normal designs. The lift coefficient then is reduced to a constant times the weight over the square of the true indicated air speed, $C_L = \left(\frac{2}{\rho_0 S}\right)\left(\frac{W}{V_i^2}\right)$.* The calibration of the pitot installation may then be plotted in the form of per cent error against the factor W/V_i^2. An equivalent plot would be one of the ratio of the indicated air speed to the true indicated air speed $\frac{V_I}{V_i}$ *vs.* the factor, the square root of the weight divided by the true indicated air speed, $\frac{W^{1/2}}{V_i}$. This is illustrated in Fig. 14. Since the angle of attack for a given lift coefficient is affected by the deflection of the wing flaps, a separate calibration curve in general will be obtained for each flap deflection.

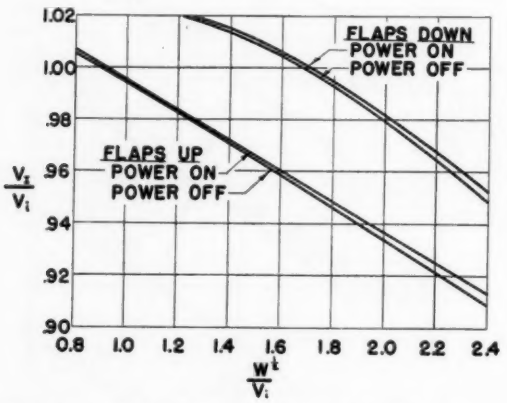

FIG. 14. Airspeed calibration, effect of power and flap position.

If the power has an appreciable effect on the lift for a given angle of attack, it will be necessary to develop air speed calibration curves for various conditions of power, including power-off. The introduction of the wing flap has considerably complicated the problem of air speed calibration. Besides that, the increasing appreciation for the effect of power has brought a realization of the added complication of power. The calibration, as plotted in Fig. 14, of course, is not directly usable. The usable form is the familiar one of the plot of indicated air speed *vs.* true indicated air speed, or, indicated correction *vs.* indicated air speed of pitot installation, and a complete calibration of this type will include a series of curves covering the range of weight, flap, and power conditions. Fig. 15 illustrates for a typical airplane, a series of correction curves for power-off, for the extreme flap settings, and for various weights.

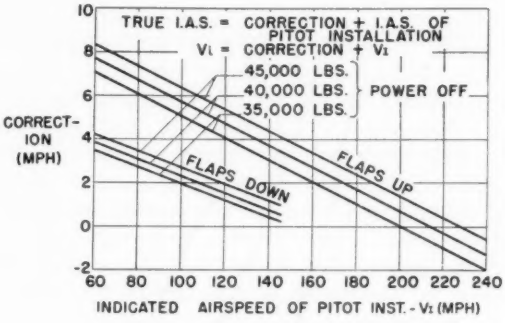

FIG. 15. Airspeed calibration chart.

B. *General Performance.* The data recorded during a flight test for performance include the basic factors of time, altitude, power, engine r.p.m., air temperature, carburetor mixture, and fuel load. These data may be recorded at regular intervals of time or altitude, or may be recorded continuously on a graph whose basic variable is time. In any case, the rate of climb is measured by the slope of the altitude *vs.* time curve. In general, this does not give a true geometric rate of climb. This is the case because the altitude, as measured by the altimeter, is not the true altitude. Recalling the definition of standard atmosphere and the means by which the altitude calibration is made on the altimeter, it is realized that the altimeter indicates true altitude only in case the pressure and temperature conditions result in a static pressure drop, below existing surface pressure, necessary to produce standard pressure at the particular altitude. However, so far as establishing a definite figure for performance is concerned, it is only necessary that the standard temperature exist for the atmospheric pressure at which the performance is determined. In other words, each individual performance figure may be corrected for temperature at the particular pressure altitude. The airplane, propeller, and the engine are not at all interested in the geometric altitude. They are interested only in the temperature and pressure so far as the atmosphere is concerned. Neglecting for the moment the effect of moisture, air currents, etc., it can be shown that the true rate of climb is obtained from the rate of change of pressure altitude by multiplying by the ratio of the absolute temperature, existing during the test, to the standard absolute temperature, corresponding to the particular pressure altitude. This relation is easily obtained from the general gas equation and the hydro-static equation for the atmosphere. The air speed calibration deter-

† For climb (or descent) a component of the weight is carried by the thrust (or drag), in which case the problem becomes more involved. For simplicity, the level case is here presented. The case of climb (or descent) is a simple extension of the case of level flight.

* For the purposes of this paper, the true indicated air speed is defined on the basis of dynamic rather than impact pressure. This definition clearly has certain advantages.

mines the true indicated air speed. The pressure altitude and air temperature determine the relative density. The fuel load determines the gross weight. The engine gear ratio and the engine r.p.m. determine the propeller r.p.m. Combining these factors with the measured power and rate of climb, the basic parameters V_{iw}, P_{iw}, N_{iw}, and C_{iw} are determined. Having determined these parameters for all of the conditions tested, a plot similar to Fig. 8 results. Because of changes in weight due to fuel consumed, changes in temperature due to time and location, and changes in power due to ram, there is no series of points that may be directly faired to form curves at constant P_{iw} and N_{iw}. The final curves that may be faired through such data result from a series of fairings, cross-plotting, and refairing, eliminating points widely in error, and applying judgment, realizing the accuracy that may be expected in flight testing. In order to illustrate this procedure, the successive steps will be described.

First of all, it is possible to approximate curves for constant P_{iw} by the simple method of sketching in by eye as the surveyor does in drawing his contour maps. This gives the first approximation. On the basis of these curves, a cross-plot may be obtained, as shown in Fig. 16, plotting C_{iw} *vs.* P_{iw} at constant V_{iw} neglecting for the first approximation the effects of N_{iw}. This cross-plot will at once reveal any gross error in contour sketching. These errors may be eliminated by a refairing of the original curves and a recross-plot. When the curves of Fig. 8 and the cross-plot of Fig. 16 are reasonable and consistent, a correction for N_{iw} may be made. The details of this process become quite involved and their explanation would be too extended for inclusion in this paper. This correction for N_{iw} roughly amounts to the following: The effect of variation of N_{iw} at constant P_{iw} is a variation in propulsive efficiency. The variation of propulsive efficiency may be closely approximated by the use of propeller charts obtained from the wind tunnel tests on an installation very similar to that tested in flight. In general, propulsive efficiency for the model tests may vary considerably from propulsive efficiency developed during the flight test. However, it is variation in propulsive efficiency with N_{iw} and not the actual magnitude of the propulsive efficiency that is desired. The variation in propulsive efficiency as obtained from the propeller charts may in general closely approximate the actual variation in flight. In any case, the effect of change of propulsive efficiency is small and any errors in calculating this effect, although even relatively large, say as much as 10 or 20 per cent, will be negligible in the final result. However, in general the propulsive efficiency correction is in error much less than 20 per cent.

Having corrected the points on Fig. 8 to certain constant values of N_{iw}, a refairing and cross-fairing process may be made to obtain the final faired results. This final fairing then represents the performance of the airplane for all conditions of speed, power, r.p.m., altitude, temperature and weight within the range tested. Within reasonable limits, extrapolation may also be made.

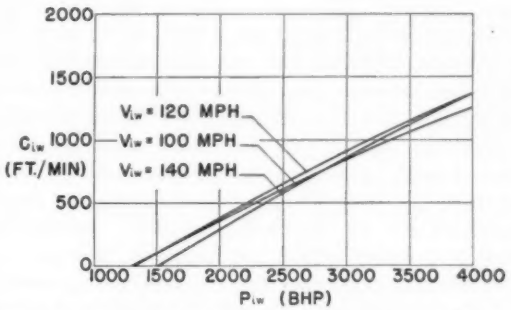

FIG. 16. Cross-plot to fair performance curves of Fig. 8.

C. *Power Calibration.* Once the data of Fig. 8 have been accurately determined, the performance for any given power may be easily determined. Whether any given power may actually be developed for given conditions depends upon the particular power plant. In order to determine whether the power plant will develop a certain power, a complete calibration in flight is necessary. The power rating of an engine, even though accurate for sea level and altitude conditions, does not in general apply to the installation in an airplane. For several reasons, the power output depends upon each particular installation. These reasons include carburetor ram or its equivalent, engine cooling, cooling distribution, mixture (which may be different from test stand conditions in order to obtain desired engine cooling or economy), carburetor air intake temperature, exhaust backpressure, accessory loads, and any other minor factors. So far as actual power output is concerned, a power calibration is not necessary for part throttle. Part-throttle power calibrations will give power, r.p.m., manifold pressure, and mixture relations, but these relations are not necessary for the simple determination of performance which does not involve fuel consumption. Obviously performance relating to range, endurance, and economy necessarily must involve power plant fuel consumption calibrations. The basic calibration necessary for the determination of the performance limit of an airplane is the full-throttle power calibration for various conditions of r.p.m., altitude, mixture, indicated air speed, carburetor air temperature, and engine cooling. (Manifold pressure is a dependent variable which results from the calibration but is not necessary for its definition.)

First, consider the power calibration at full throttle at best power mixture. In order to obtain this calibration, it is necessary to obtain power at full throttle throughout the operating range of r.p.m. and altitude at the best power mixture. It is also necessary to obtain carburetor intake pressure as affected by ram for all of these conditions. The carburetor intake ram is

normally a function of true indicated air speed, weight, power, and density. The true indicated air speed is a major factor determining the pressure field about the airplane, and hence the pressure at the carburetor intake. The true indicated air speed and the weight determine the angle of attack. The power output and the density determine the rate of intake airflow, and hence the pressure drop through the intake system. For a simple short-ducted carburetor intake, the effect of power on pressure drop may be negligible. The effect of weight depends upon the wing loading and the weight range. For the majority of designs this weight effect also may be essentially negligible. In case the power and weight effects are negligible, a single carburetor intake ram curve may be developed as a function of true indicated air speed. The intake ram calibration curve may be obtained and plotted as in Fig. 17. Another factor which may be applicable is that of flap deflection. The effect of flaps is to change the angle of attack for a given indicated air speed. Normally the condition of flaps deflected is not considered of importance because prolonged operation with flaps deflected is unusual.

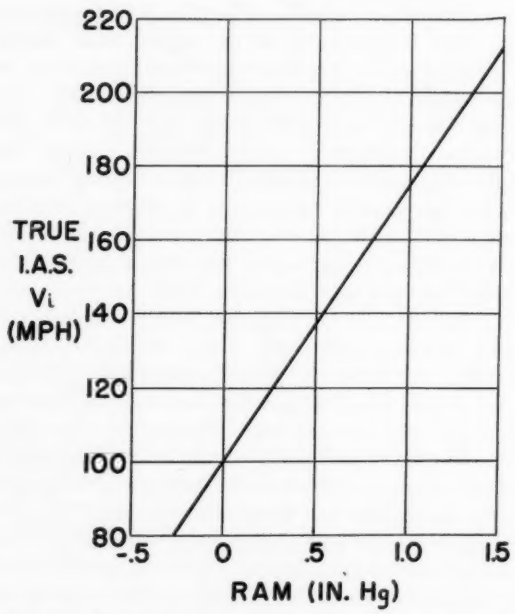

FIG. 17. Variation of carburetor ram with true indicated airspeed.

At full throttle the power output at a given pressure altitude is affected by the air temperature in two ways: First, the air temperature affects the density of the air entering the supercharger. The pressure rise through the supercharger is a function of this density. Hence, the pressure of the charge entering the engine is a function of the density of the air entering the supercharger. Second, the density of the air entering the engine is also a function of the temperature. The power at full throttle obtained under one condition of temperature at a given pressure altitude may be corrected to any other temperature by means of two corrections. The first involves a correction of the pressure rise through the supercharger and the second is a correction of the density of the ingoing charge. Curves of the form of Fig. 18 have been developed for temperature correction of manifold pressure. Having obtained during the power calibration data on the relation between the density of the entering charge and the pressure rise through the supercharger, the pressure rise through the supercharger for any other intake temperature condition may be determined. It is therefore possible to obtain a series of curves at various engine r.p.m.'s, showing pressure rise through the supercharger as a function of carburetor inlet pressure at a given atmospheric temperature, as in Fig. 19. This serves as a pressure calibration of the supercharger. The power output of the engine at a given pressure of the charge entering the engine depends upon the temperature of that charge. This temperature in general is a direct function of the temperature of the atmosphere. A relation which has been established for some time and which proves to be sufficiently accurate is that the power output of the engine is inversely proportional to the square root of the absolute temperature of the atmosphere.

The two temperature corrections, one for pressure rise through the supercharger and the other for the density of the charge entering the engine form the temperature power correction necessary for the power calibration.

Because the air intake system of a power plant is of necessity close to a source of heat, the temperature of the air may be raised above that of the free air. Any rise in air temperature from this cause will cause loss in power as compared to that which would be developed were there no rise. However, such temperature rise normally is small and does not affect the method of power calibration. It appears only as a defect in the power plant installation that acts as one of several factors to reduce the power output as compared to test stand calibration.*

Because of the latent heat absorbed by the rapidly vaporizing fuel, the region after the carburetor is an excellent refrigerator under certain circumstances of carburetor design, power, throttle, and outside air temperature. If the air carries sufficient moisture as vapor or moisture in proper quantity as droplets, ice may be deposited on the duct walls. The ice deposit may grow to such an extent that it completely chokes off

* This method differs from that in *Aircraft Engine Power Estimation from Intake Manifold Density* by Rhines, Thomas B., and Schipper, Peter W., Journal of the Aeronautical Sciences, Vol. 6, No. 3, page 106, January, 1939, because of its purpose. Its purpose is to develop an engine calibration easily usable with airplane flight test performance reduction. The purpose of the method of Rhines and Schipper is to develop a basic method of study of engine power at altitude usable basically for engine performance.

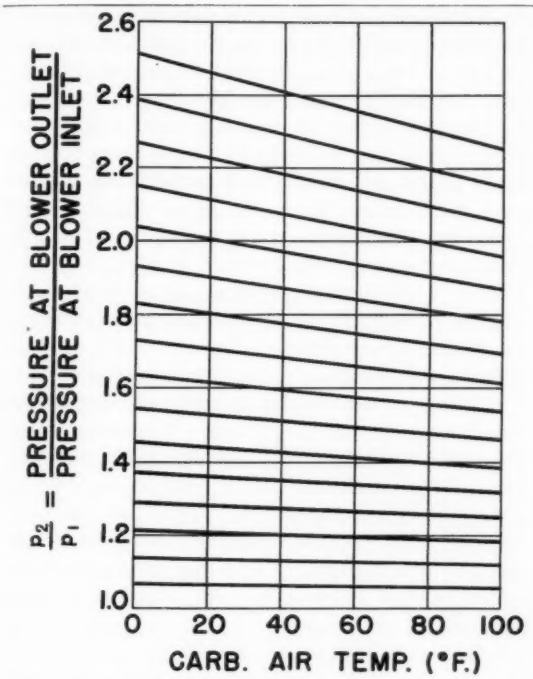

FIG. 18. Manifold pressure correction for carburetor air temperature.

the intake. This ice formation must be prevented in some manner. The usual method is to provide a means of heating the intake air. Generally such a provision not only raises the temperature but acts as a choke and reduces the intake pressure. For some carburetor installations for which preheat operation is not unusual, a power calibration with the preheat on may be necessary. Basically this is no different from the normal calibration for cold air.

Another power correction which is necessary in obtaining a complete power calibration is that for mixture of the intake charge. Normally the primary power calibration of an engine is made at the mixture for best power. For mixtures appreciably richer or leaner than best power mixture, the power is measurably reduced. The effect of mixture on power is essentially independent of altitude. It is also independent of temperature so long as the detonation limit is not reached. Hence, normally it is sufficient to obtain the effect of mixture on power throughout the operating range of power and r.p.m. without particular regard to temperature or altitude. The plot of Fig. 20 illustrates the effect of fuel/air mixture on power.† If the detonation limit is reached the leanest mixture is determined by the atmospheric temperature.

Having established the principles by which the power

† Good accuracy in measuring fuel/air ratio is obtained if the instrument is serviced and calibrated before and after each flight. Otherwise, fuel/air ratio measurements may be of very doubtful accuracy.

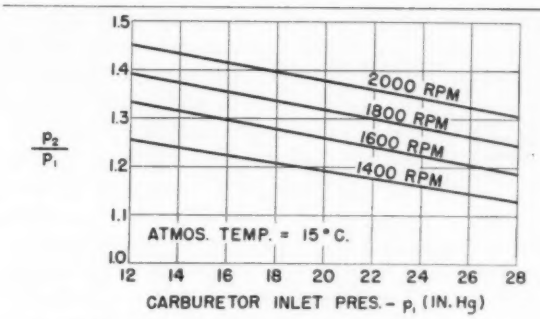

FIG. 19. Pressure calibration of engine supercharger.

calibration is obtained, it would be of value to follow the steps of obtaining actual power calibrations. First, of course, the power data must be obtained in flight tests for the atmospheric conditions existing at the particular time. From this data, power curves may be developed for any of the series of temperature conditions in the atmosphere. The actual power obtained at any particular point may be corrected to a desired indicated air speed by means of the intake ram calibration and the supercharging pressure rise calibration. The use of these two calibrations gives the correction to the pressure of the charge entering the engine. How the power is affected by the pressure of the charge is determined from the relation between so-called manifold pressure and power. This relation may be determined either by tests on the ground or by tests in the air Normally, the first is available from the engine manufacturer's power calibration of the engine and the second is available from the power calibration in flight. One offers a check against the other. The relation between manifold pressure and power is illustrated in Fig. 21. Now, having determined the power output at a given indicated air speed, the next step is to obtain the power at a given air temperature. First, a correction for manifold pressure is necessary and is obtained by means of the curves of Fig. 18. Second, a correction for density of the charge entering the engine is necessary and is obtained by means of the relation that power is inversely proportional to the square root of the absolute temperature of the atmosphere. Having corrected a series of

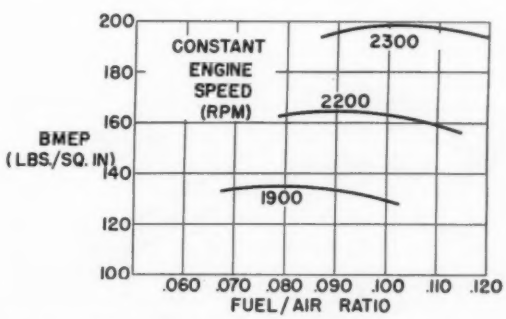

FIG. 20. Effect of mixture on power for constant engine r.p.m., throttle and altitude

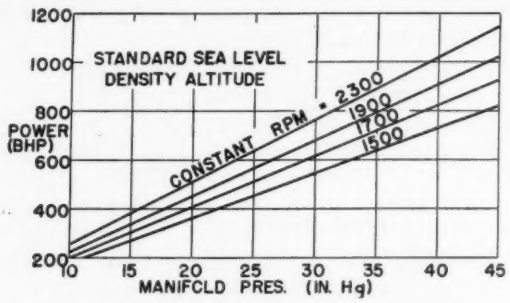

FIG. 21. Variation of engine power with manifold pressure for constant r.p.m.

points in this way at various altitudes at full-throttle and at a given r.p.m., it is possible to plot a curve of full-throttle power *vs.* altitude for a given condition of indicated air speed, r.p.m., and atmospheric temperature. A series of these curves may be obtained for the range of operation. Such a plot is illustrated in Fig. 22. Having obtained such a complete power calibration, it is a simple process to determine the performance of an airplane by means of the charts of Fig. 8 and Fig. 22. Thus, by means of two such complete charts, the entire performance of an airplane may be presented for operation at best power mixture. For operation at mixtures other than best power, a correction for power by means of a series of curves, as in Fig. 20, will be necessary. Two primary curves supplemented by the mixture curve then present the full range of performance of the airplane for normal flight. A number of factors have been neglected in reducing the data in this manner. Among these factors are Reynolds Number, the effects of compressibility on the aerodynamics of both the airplane and the propeller, the variation in power output from engine to engine, the variation in power output during the life of the engine, and other such factors. The use of the torquemeter will eliminate the power variation problem.

THE TECHNIQUE OF HANDLING THE AIRPLANE FOR PERFORMANCE TESTS

Few other fields of engineering measurement offer so many possibilities of error as the determination of airplane speed and climb-rate. In the past the precision of such tests has sometimes been so bad that results could not be relied upon within 10 per cent because of lack of weight control, improper instrumentation, uncontrolled technique, or failure to evaluate the variables involved in the measurement of performance. When modern methods and technique are available a flight test accuracy of ± 1 per cent can be realized in measuring both climb-rate and velocity.

The principal factors requiring careful control in flight testing are (1) weight control such that the gross weight of the airplane can be determined at any time during the test, (2) instrumentation provided in advance so as to give accurate measurements of every element vitally affecting the space-energy picture, (3) drag control so that parasite resistance does not change in some unknown manner during the test, (4) restriction of testing to known atmospheric conditions, particularly eliminating vertical air currents, (5) maintenance of steady conditions of flight long enough to assure stabilized energy relationships, and (6) experience in the type of precision flying required for testing.

Weight control requires accurate weighing and subsequent checking of all items added or subtracted from the airplane. Primary on all large aircraft is the item of fuel used during the flight. The difference in weight between the start and end of a flight test will often be enough, if uncorrected, to make otherwise excellent results inconsistent and unreliable. On each flight, a data sheet is maintained for the purpose of keeping a running time-log of the gross weight of the airplane. Fuel consumed can be read from fuel gages from time to time, and weight computed from these figures and checked at the end of the flight. Such a log and its accompanying chart of weight *vs.* time are shown in Fig. 23. Each reading of velocity and climb can then be corrected for the proper ratio of gross weight to standard gross weight.

Instrumentation for tests requiring accuracy can be done properly only when it is begun prior to the beginning of the test, preferably prior to completion of the airplane. The principal performance instruments requiring careful selection, calibration, installation, and

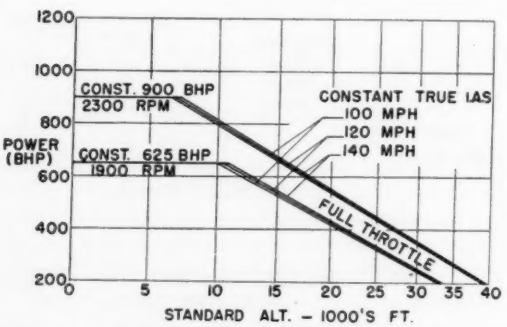

FIG. 22. Power calibration chart.

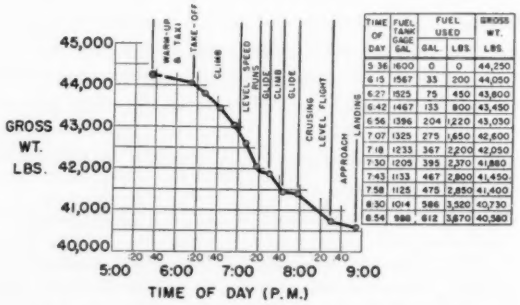

TIME OF DAY	FUEL TANK GAGE GAL	FUEL USED GAL	FUEL USED LBS.	GROSS WT. LBS.
5 36	1600	0	0	44,250
6 15	1567	33	200	44,050
6 27	1525	75	450	43,800
6 42	1467	133	800	43,450
6 56	1396	204	1,220	43,030
7 07	1325	275	1,650	42,600
7 18	1233	367	2,200	42,050
7 30	1205	395	2,370	41,880
7 43	1133	467	2,800	41,450
7 58	1125	475	2,850	41,400
8 30	1014	586	3,520	40,730
8 54	988	612	3,670	40,580

FIG. 23. Weight vs. time for a typical flight test.

attention are (1) the air temperature gage, (2) the sensitive altimeter, (3) the air speed indicator, (4) the tachometer, (5) the torquemeter, (or in its absence the manifold pressure gage, the carburetor air temperature gage, the mixture indicator and engine temperature indicators).

Atmospheric temperature is a very difficult measurement to make accurately. Small errors in this measurement are equivalent to excessively large errors in density altitude and air speed. In order to show this effect, the following table has been made:

Common Error	Error Introduced by Temperature Error
Air Temp.—±10°C. for improper measurement	
Air Press.—±20 ft. on std. sensitive alt.	±1200 ft.
Air Speed ±1 m.p.h. on test instrument	±3.5 m.p.h. at 200 m.p.h.

Common errors in obtaining air temperature accurately introduce errors in altitude 60 times the commonly obtained accuracy of making this reading and $3\frac{1}{2}$ times the commonly obtained accuracy in obtaining air speed.

It is clear from this that the principal effort should be placed upon reducing the usual error of temperature measurement by a large amount in order to equal the accuracy of other important measurements. An accuracy of ±1°C. is desired at the present state of the art. Indicated temperature differences as great as 35°C. have been noted on an airplane in flight on different thermometers whose elements were located at various points on the airplane.

There are several primary reasons for the excessive error in obtaining air temperature. One of these is the location of the thermometer element at a point where it will not measure the true air temperature at the altitude of the test. The element may be picking up heat from the engine or from the slipstream of the propeller or from the sunlight (either direct radiation or conduction of heat from surrounding sun-heated surfaces) or from adiabatic temperature changes owing to compression or expansion at localized points around the airplane. The avoidance of the engine, propeller, and sunlight effects is readily obvious. Elimination of the errors due to adiabatic heating can be accomplished in one of several ways. Since compression effects upon temperature are virtually non-existent at speeds under 100 m.p.h., the airplane can be flown slowly at the altitude in question long enough to get stabilized temperature readings. An experimental correction can easily be determined which can be used for this purpose if the temperature element is normal to the airstream. Some test personnel prefer to make the temperature reading from a separate slow flying airplane sent up for the purpose of obtaining the altitude-temperature gradient at the time of the test.

Lag effects are quite serious in climbs and descents where the temperature indications may be several degrees behind the actual temperature at any instant during the changes in altitude. These effects can sometimes be satisfactorily reduced on slowly climbing airplanes by measuring temperatures during both climbs and descents made at the same rate of change of altitude.

Thermocouples have been found to be more satisfactory than resistance type elements for measuring outside air temperature owing to the difficulty of correcting the latter for the effects of changes in rates of radiation in air of varying density. When this element is normal to the airstream it is subjected to total pressure developed by the velocity of the airplane.

When so installed, a simple experimental correction can be made for the rise in temperature due to compression. If the element is not normal to the airstream, the correction becomes involved by local pressures.

Accurate pressure instruments for measuring pressure altitude are now available so that this measurement should be the easiest of all to obtain within the desired accuracy. The standard cockpit sensitive altimeter is perfectly satisfactory for determining pressures if properly calibrated and installed. It must, of course, be vented to the static tube of the air-speed pitot in order to establish a standard. Of course this standard must be calibrated in the same manner as the air speed to eliminate errors due to local pressures.

A special air-speed indicator is desirable for performance testing primarily for convenience and saving of flight test time. Graduations in one m.p.h. intervals are desired. The calibration of this instrument is made separately in addition to the calibration of the complete air speed indicator installation. Then, when a new instrument is used for replacement, it will be unnecessary to recalibrate the airplane.

The simplest form of air-speed indicator calibration is made by flying the airplane at its full gross weight, at very low altitude, across a measured course at constant indicated air speed, and timing the runs for a distance great enough to reduce the error of measurement to a value consistent with the error of other flight test measurements. When the airplane is flown across such a course both up-wind and down-wind a sufficient number of times throughout the speed range required for the calibration, a curve can be drawn of indicated air speed *vs.* true indicated air speed. With the usual instruments, such a method of calibrating the air speed indicator involves, however, so many and such large errors as a rule that it is not feasible for accurate flight testing unless ideal conditions are available. An automatic timer of high accuracy allows the use of this method over a short course of a few hundred feet. In such a short distance variation in some of the factors is minimized. But even so, the wind conditions must be very consistent or constant.

One modern method of air-speed meter calibration is

the use of a trailing bomb. A trailing bomb is a pitot tube mounted in such a manner in a streamlined, finned body, that it can be trailed below and behind the airplane in a region undisturbed by the airflow around the wings or body. The disturbance has been found to be less severe behind and below than directly below the airplane. This fact fits well with the trailing position of the bomb hung by a cable from the rear of the airplane body. The cable carries the tubes transmitting the pressures from the pitot to the airplane air speed indicator. Cloth streamers are tied at intervals to the cable to give the desired trail angle and bomb position with respect to the airplane. A cable length at least equal to one span should be used, and the bomb should be lowered from a point as far aft as possible.

The calibration of an air-speed meter installation with a trailing bomb may be accomplished at any altitude. The bomb is first calibrated in a wind tunnel, from which a relation between indicated air speed and true air speed is determined.

The calibration technique consists in obtaining at a series of air speeds throughout the speed range simultaneous readings of two air speed indicators, one of which is connected to the airplane's pitot-static and the other connected to the pitot-static of the trailing bomb pitot. Care is necessary to avoid trailing the bomb in air of velocity different from that at the airplane level. Also, unless the airplane and bomb pitot and static lines are properly balanced for changes of pressure, the trailing bomb air-speed calibration must be performed in level flight.

Of primary importance in measuring performance, both climb-rate and speed, are the instruments dealing with the power available at various altitudes and attitudes of the airplane. The tachometer is now sufficiently developed and standardized as to give results well within desired flight test accuracy. There are, however, a number of tachometers on the market whose accuracy should be accepted with caution. Until torquemeters came into use for flight testing, measurements of torque had to be made indirectly from readings of intake manifold pressure, carburetor air temperature, fuel mixture strength and other variables entering into the determination of b.m.e.p. The methods of accomplishing this are explained above in the section dealing with engine calibration.

The instruments themselves offer no serious difficulty from the viewpoint of calibration and interpretation. All instruments should be re-calibrated at intervals in order to assure their accuracy. An able man assigned to the instrument problem can easily save large losses arising from uncontrolled instrumentation.

The problem of drag control should be so obvious as to require no comment. It is, however, a problem to be watched carefully. The best means of watching it during development tests of a new airplane has been found to document each flight very completely from the viewpoint of changes occurring to the external characteristics of the airplane. During flight notations may be made frequently of cowl flap position, landing gear position, or any other variable which might affect flight characteristics.

The atmosphere is a sea of air in which man has, after many years, managed to navigate unsupported by solid connection to the earth or by means of any appreciable buoyancy of simple displacement. This sea is not quiescent but is ever in a turmoil under the forces of thermo- and aero-dynamics that visibly produce our weather. It may flow as a tumbling waterfall over the mountainous areas or become a turbulent, rolling, seething mass, or flow smoothly and quietly with unappreciable ripple. The air currents may be made visible by the clouds they produce, or by the smoke, dust, soil, and sand that they lift and carry. Even if visible, the magnitude of their effect is not directly apparent. Visible or not visible, the effect of air currents has been frequently ignored in determining airplane performance.

The effect of air currents upon the accuracy of performance tests can be figuratively disastrous. The way in which air currents affect the performance of an airplane is well illustrated by the feats of soaring. We might well investigate some quantitative figures of air current effects.

(1) *Vertical Currents.* Vertical currents are those by which thermal soaring is possible. A vertical current adds directly, vectorially, to the rate of climb. In level flight the speed is changed by that amount necessary to produce a vectorial sum of zero. For example, in Fig. 2, one may quickly determine the change in level speed for a descending current of 500 ft./min. by finding the difference between normal level speed and the speed for 500 ft./min. rate of climb for the given conditions of power, weight, and altitude.

A vertical current may have a horizontal gradient. Its effect may be appreciable.

$$\frac{W}{g} \times \frac{dw}{ds} \times V \times V = W \times \Delta C$$

$$\frac{\Delta C}{V} = \frac{V}{g} \times \frac{dw}{ds}$$

where

W = airplane weight
g = acceleration due to gravity
w = vertical current
s = horizontal distance
V = air speed
ΔC = change in rate of climb

If the horizontal gradient is 1.61 ft./sec. (about 100 ft./min.) per 1000 ft. for an airplane flying at 200 ft./sec. (about 140 m.p.h.), the rate of climb is increased by 1 per cent of the air speed or 120 ft./min.

(2) *Horizontal Current.* A horizontal current of constant magnitude with respect to all axes adds simply vectorially to the ground speed but has no other effect.

If a horizontal air current has a horizontal acceleration of given value, the airplane performance may be measurably affected. Taking the wind velocity and airplane velocity positive in the same direction, a positive wind acceleration will decrease the airplane performance. This is true since the airplane performance depends on its momentum with respect to the surrounding air. If the air current is continually increasing, the airplane finds itself struggling to maintain its momentum with respect to the air. In other words, it spends part of its thrust in accelerating with respect to the ground. This required acceleration might be expressed in equivalent rate of climb.

$$\frac{W}{g} \times a \times V = W \times \Delta C$$

$$\Delta C = \frac{a}{g} V$$

where

a = acceleration of air current

A horizontal acceleration of $1/10g$ changes the rate of climb of an airplane flying at 180 ft./sec. (about 120 m.p.h.) by 1080 ft./min. A horizontal acceleration might easily give the impression of a strong vertical current.

A vertical gradient of a horizontal current does not affect level air speed but may very appreciably affect rate of climb. An airplane climbing in a current of such gradient is in the same position of an airplane flying in an accelerating current of zero gradient. If the vertical gradient is positive, the airplane has to exert itself to maintain its air speed.

$$\frac{W}{g} \times \frac{dw}{dh} \times C \times V = W \times \Delta C$$

$$\frac{\Delta C}{C} = \frac{V}{g} \times \frac{dw}{dh}$$

where

h = vertical distance
C = rate of climb in still air

For a vertical gradient of 16.1 ft./sec. per 1000 ft. for an airplane flying at 200 ft./sec. (about 140 m.p.h.) the rate of climb is reduced by 10 per cent.

An angle of yaw on the air-speed pitot may introduce quite an appreciable error into the air-speed indicator readings. When the air-speed pitot is located in such a position relative to the wing or body that flight at an angle of yaw influences the pressure distribution in the region of the pitot head, the error introduced by yaw is even greater. Errors of ± 4 m.p.h. are not uncommon for barely appreciable angles of yaw on some aircraft. For steady level flight, the air speed for a stabilized zero-yaw condition will be different from that at a yawed-flight condition, primarily because of the fact that the airplane is sideslipping and must therefore be held in a climbing attitude in order to maintain the same altitude. For all of these reasons, it is quite necessary to maintain zero angle of yaw. This can be done either with a yaw meter, or for essentially symmetrical conditions, by means of the standard turn and bank indicator or artificial horizon.

Unless the test pilot has a definite knowledge of the precision necessary in taking readings of his various instruments, he cannot arrive at a satisfactory precision with the most economical use of his time. It is not always possible to wait until the atmospheric conditions are perfect before making a flight test. It is also not always possible to throw out flight tests in which vertical currents were encountered. The great cost of flight test time requires that the test pilot determine the minimum time required to obtain the desired accuracy. For level flight readings, it should be possible to obtain an accurate reading of $\pm$ one-half per cent. It should be possible to repeat flight tests and get results with this degree of precision. Due, however, to the large number of variables which cannot always be brought under control from day to day, any comparison of speeds made for the purpose of obtaining drag indications must be made over a full range of power output. This is especially true when torquemeters are not available.

Due to the very large differences in lag and sensitivity of the cockpit instruments, it is essential for accurate performance measurements to guide the technique of piloting by means of the proper sequences of instrument reading. It is frequently impossible, for instance, to fly in any given steady attitude by means of the rate-of-climb meter because of its lag and enormous variability with airplane angular velocity. It is virtually impossible for a pilot to guide a transport airplanes' descent by the rate-of-climb meter alone. It is necessary in this case to determine the approximate air speed which gives a given average rate of descent, and then change this air speed in accordance with the average indications of the rate-of-climb meter by a trial and error process until the desired rate of descent is obtained.

This technique can be acquired only by practice in obtaining the desired stabilized conditions. It is for this reason that testing of performance with a pilot not trained in test flying is a very wasteful process from the point of view of flight test time and flight test accuracy.

The Testing of Climb Performance

The flight tests for determining climb performance require the control of weight throughout the flight, as explained above, so that the instantaneous weight can be used for climb-rate reduction. A continuous record of fuel load is necessary in order to prepare the plot of gross weight *vs.* time from calculations which are made to obtain the coordinates C_{iw} and V_{iw}. The layout of the flight plan is based upon the principle that optimum climb-rate may be determined by a series of short steady

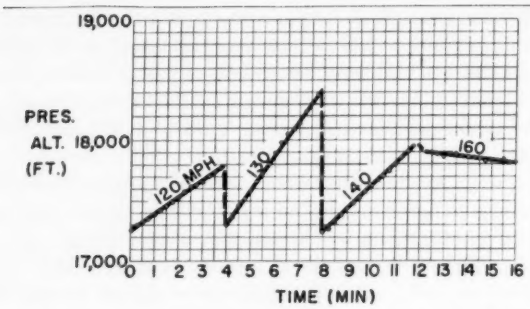

FIG. 24. Observed climb-rate for various constant indicated airspeeds.

climbs at predetermined air speeds and powers. The air speed chosen shall bracket the speed for best climb-rate. The chart of altitude *vs.* time for such a test will have the appearance of a sawtooth, as in Fig. 24. The slope of the climb portions of the record give the rates of climb at the altitude past which the steady climb attitude was maintained. Frequently it is possible to obtain greater accuracy than the barograph record can give by having an observer make a continuous plot of altitudes at 15-second intervals. The standard sensitive altimeter is more accurate than the usual flight test barograph. Its use also offers the advantage of enabling the observer to discard portions of the climb obviously affected by vertical currents or by inaccurately maintained velocity observable while plotting results.

Constant power is maintained in climbs made below critical altitude or at partial powers to be used in the density climb-rate curve of Fig. 16. Sawtooth climbs are required at several altitudes and at a sufficient number of air speeds in order to insure (a) that best climb-rate speed has been bracketed and (b) that an accurately formed curve of velocity *vs.* climb-rate is obtained in the region of best speed. Sawtooth climbs at reduced power are necessary in order to determine the full range of climbing ability of the airplane.

On multi-engined aircraft, climbing performance for one or two engines inoperative is determined by making sawtooth climbs under the desired conditions. For an accurate determination of ceiling with one or more engines inoperative, sawtooth descents above ceiling are desirable, and rates of descent under the steady conditions are determined in the same manner as the rates of climb were determined.

The so-called check climb, frequently made to check upon the accuracy of the sawtooth climb-rate determinations, is actually an unnecessary flight since it determines, as a rule, not the climbing ability of the airplane, but the average accuracy of the pilot who makes it. Comparisons between airplanes made by comparing check climbs made by different pilots are seldom accurate engineering measurements.

Below critical altitude the "rated-power" climb will have a similar shape to the constant-power climbs throughout the density-altitude climb-rate chart. Cruising-power climb is a characteristic curve that is very useful for all airline work. In fact, rate-of-climb *vs.* density-altitude curves for various cruising powers are needed in order to complete the picture of airline performance. Full-throttle rate-of-climb curves can be drawn for various temperatures above and below standard. This will complete the picture of the full range of climb performance.

When best angle of climb as well as best rate of climb is desired, as it is for take-off power, rates of climb should be determined at several velocities less than the velocity for best climb-rate. The curve of climb-rate *vs.* velocity can be extended downward to the point of tangency of a line drawn from the origin. This point of tangency defines the speed for best angle of climb. This is primarily important only for take-off power, where obstacle clearing ability is to be determined.

It may also be important to have rates of climb determined accurately for speeds higher than the speed of best climb-rate. These rates of climb are useful in determining airline operating flight paths where cruising climbs are carried out at higher speeds in order to get the maximum distance covered in a given length of time for the first part of the airline flight.

The traditional method of determining rates of climb from the power-required curve and the power available relationship is illustrated in Fig. 25. Excess power here assumes a static condition of the power-required curve.

As was pointed out in the section on the generalized conception of performance, this conception of "excess power" is an approximation. The power-required curve is not representative for all conditions of power; generally it is the level-flight power-required curve that is determined. Accurately, there will be a series of power-required curves throughout the range of applied excess powers.

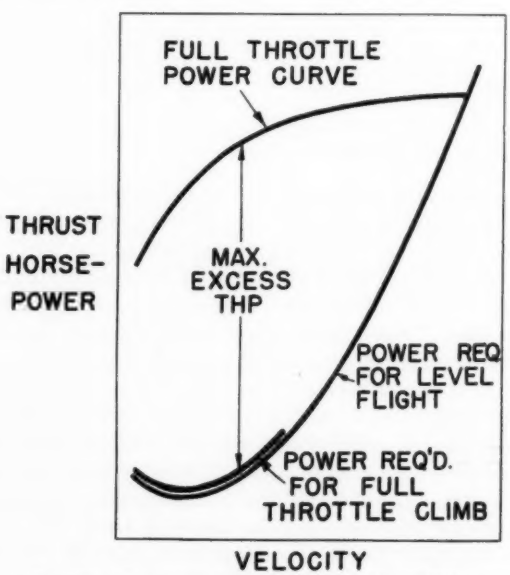

FIG. 25. Power required for climb and level flight.

An important factor in making the power required for climb differ from that required for level flight is that at constant indicated air speed in a climb, the true air speed is increasing. This increase in air speed is acceleration that requires thrust to produce. Therefore, in a climb at constant indicated air speed (or at any changing indicated air speed that corresponds to changing true air speed), additional power is required for acceleration.

Velocity in Level Flight at Various Powers

A determination of level flight speeds, at various altitudes, powers, gross weights, propeller r.p.m., engine b.m.e.p., and fuel flows, is a very important part of the flight test program. In it the principal correlation between wind tunnel and flight test is determined. If the airplane is equipped with torquemeters, this determination is greatly simplified, and the accuracy is greatly improved. It requires, nevertheless, very careful instrumentation and technique. It also requires careful control of weight, since there is frequently a very large difference in the level speed at any altitude for different gross weights. Cruising speed is, of course, to be plotted against density altitude, and the simplest form of such a plot is shown in Fig. 26 where pressure altitude and atmospheric temperature determine the density altitude for use throughout the velocity chart. On such a density altitude basis, velocities for

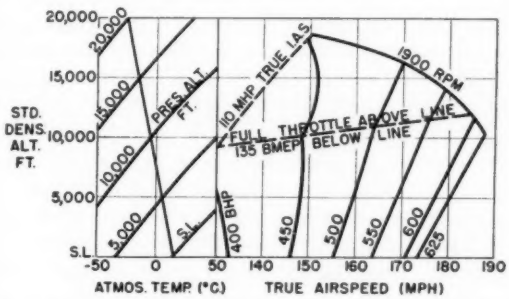

Fig. 26. Cruising power chart 45,000 lbs. gross weight.

constant power can be accurately plotted up to the full-throttle conditions. Full throttle will not occur at the same point in this chart if the atmospheric temperature varies from standard. It is, however, possible to draw full-throttle lines for constant variations from standard temperature.

On airplanes equipped with fixed-pitch propellers, or with two-position controllable propellers, or with propellers having a pitch-angle indicator, cruising charts can be drawn showing the velocity relationships for constant propeller r.p.m. and constant power, and at the desired propeller blade angle. The propeller r.p.m. lines will appear, in this case, as in Fig. 27. This forms a very satisfactory method of cruising control on small airplanes, or on those without elaborate instruments.

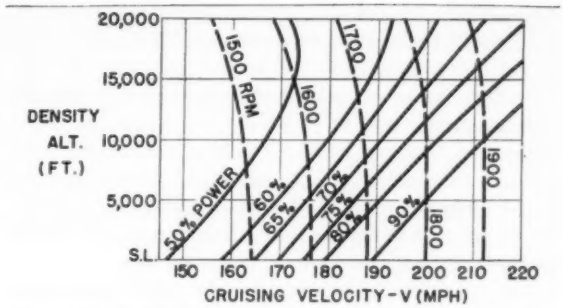

Fig. 27. Cruising power chart for airplane equipped with fixed-pitch propellers.

For airplanes having constant-speed propellers, it is preferable to draw cruising charts with constant values of b.m.e.p. since the speed can be altered to give the desired b.m.e.p. for any power. The advantage of operating at constant b.m.e.p. is that in this condition the operating severity on the engine remains at a fixed determinable value. Another advantage is that specific fuel consumption can be determined quite accurately and maintained at any desired value. On such a chart it is possible to draw lines of constant power which are also lines of constant r.p.m. and fuel flow. From these lines it is simple to determine range, and lines of constant miles per gallon can then be superimposed upon this chart. This is illustrated in Fig. 28.

The use of charts of the nature of Figs. 26, 27, and 28

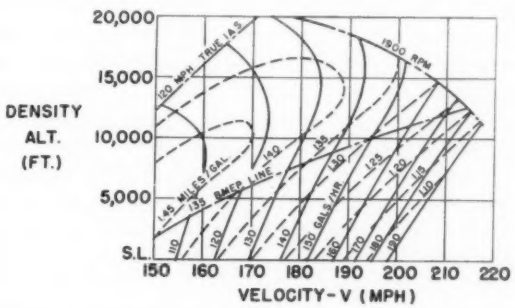

Fig. 28. Cruising fuel consumption and range chart.

for the purpose of cruising control, requires torquemeters, power calculations, or air-speed correction calculations, or their combination, depending on the accuracy desired or justified.

It may be well to note that in Fig. 26 there is a sharp change in the nature of the curves of constant power above the full throttle line. This is caused by the change in propulsive efficiency due to the increase in r.p.m. necessary to maintain constant power.

Discussion

The situation, so far as flight-test performance, flight testing, and reduction are concerned, is not so well settled as might appear by the facts presented in this paper. The methods presented here have been de-

veloped only for the simple gear-driven supercharger. For some time development work has been progressing on exhaust-driven turbo superchargers. The factors that affect the power output of such an installation are more numerous and more involved than for the gear-driven supercharger. Some excellent testing has been done on the ground. Other testing has been done and is being done in the air. The evaluation of all of the factors involved has not yet been determined and will be the basis of extensive research in the future.

The use of the hydraulic drive for remote drive and for gear reduction is now on the horizon. Its regular service use appears not too far in the future. For present engines there is a direct relation between the engine speed and the propeller speed. The introduction of the hydraulic drive will eliminate this simple situation. Another factor of complication will be introduced into the reduction and interpretation of airplane performance.

The variable area wing is now being used. How far developments along this line will go is not immediately apparent. The use of any normal wing flap, and in particular the Fowler flap, allows essentially a change in the wing area. Therefore, the performance of an airplane with a variable area wing will be handled in the same way as the performance for various wing flap settings.

The constant trend toward increasing speeds has already brought airplane performance into the outer fringes of the effects of compressibility. The entire development of the methods presented in this paper has essentially neglected the effect of compressibility of the atmosphere, except insofar as minor corrections may account therefor. In other words, the atmosphere has been treated essentially as an incompressible fluid. When the local velocity of any part of the airplane or propeller reaches the speed of sound for the air at the particular locality, the air flow takes on a sharp change in character, and it results in extremely great changes in lift and drag. This compressibility effect may be avoided by proper aerodynamic design up to a certain point. As aerodynamic design resources are exhausted and airplane speeds increase, it eventually becomes impossible to completely avoid the effects of compressibility on all parts of the airplane. These effects of compressibility do not lend themselves to the simple laws that have been used in the development of the methods in this paper. The complete answer to the question on how this effect will be handled in the interpretation and reduction of airplane performance does not appear immediately.

The method of obtaining, presenting, and reducing flight test performance data at altitude that has been covered by this paper gives a means of checking the accuracy of each point against all of the other points. The data obtained at any given altitude are not considered as data separate and by themselves. They are considered in relation to all of the data obtained at all of the altitudes tested. By this means the inaccuracies of any individual point are reduced to a minimum. A principle that may be used in preparing the data, one that is the basis of the scientific method, is that of checking the data against theory. By checking the theory against the flight test and flight test against the theory, it is possible to obtain a rational shape to the curves that are faired to the data. Having obtained a reduction of the data that is consistent with theory, it is possible to interpolate very accurately for any condition of weight, power, altitude, and temperature and extrapolate with good accuracy and to within reasonable limits. Thus, the complete performance of the airplane at all weights, powers, altitude, and temperatures may be obtained by means of specific tests at particular altitudes covering the operating range. The variations in performance with weight, power, and temperature are obtained on the basis of theory. This method applies not only to the normal conditions of flight, but applies equally well for flight with one or more engines inoperative. In case the power available is unsymmetrically placed because of failure of one or more engines, the power required is so greatly affected by the axes of thrust that the determination of performance of the airplane for all conditions of weight, power, altitude, and temperature would be an endless process of empirically collecting the data, were it not for the correlation of the data with and by the means of theory. This method then is very excellently adapted to the flight test performance of airplanes within the present normal speeds.

The Column Strength of Closed, Thin-Walled Sections of 18–8 Stainless Steel*

HOWARD W. BARLOW
New York University†

SUMMARY

Thin-walled members having closed cross-sectional shapes are used as columns in aircraft construction. The purpose of this investigation was to determine and evaluate the factors influencing the behavior of such columns fabricated from 18–8 corrosion-resistant steel. Approximately 300 specimens comprising two different cross-sectional shapes in nominal thicknesses of 0.006 in., 0.008 in., 0.010 in., 0.012 in., 0.014 in. were tested as columns under flat-end and under pin-end conditions.

In order to carry out this investigation it was necessary to develop new methods which were found to have broad application.

Two new types of special fixtures were developed which permitted pin-end tests to be conducted with the use of flat-end specimens.

A simplified and improved technique was developed for testing the columns. This technique is superior to that currently employed which makes use of imbedding plates, of cast ends and of specimens subject to loading in prior test. The technique includes an improvement in the process of preparing the samples for test.

The specimens investigated were obtained from the stock of a commercial manufacturer and had been made from two flanged channels by the shot-welding process. The channels, in turn, had been produced by the draw-bench method and were of full-hard, 18–8 chrome-nickel, corrosion-resistant steel. This material is austenitic at room temperature and cold working increases its strength, hardness and modulus of elasticity, and raises its proportional limit. The fact that the physical properties of the material are subject to change with cold working makes it necessary to determine the basic strength characteristics of the material after all processing has been completed.

The compressive elastic properties of the completed sections were determined by the use of the "Plug" method.[15] This method permits the determination of the compressive stress-strain relationship for any hollow, thin-walled section up to values of average unit stress considerably greater than those at which secondary failure usually occurs.

The column tests were analyzed on the basis of the compressive elastic properties of the material. For the sections investigated herein it was established that in the equation for primary failure by translation, the tangent modulus in compression represents the effective modulus.

The coefficient of end-fixity for flat-end column tests was found to be 4.0.

The system of non-dimensional coordinates advocated by W. R. Osgood was used in plotting the data from the compression stress-strain tests and the data from the column tests. The results for all gages of both cross-sectional shapes were found to lie on identical curves.

It was established that the critical unit stress for secondary failure is directly proportional to R and is inversely proportional to the square of the flat-pitch ratio. R is defined as a section constant for any given shape. The value of R does not vary with the thickness of the material and may be determined for each section by compression tests of a few short specimens.

Received November 9, 1940.

* Abstract of thesis submitted in partial fulfillment of the requirements for the degree of Doctor of Engineering Science, College of Engineering, New York University.

† On leave from University of Minnesota.

INTRODUCTION

In order that the stainless steels used in aircraft construction may be able to compete with the lighter alloys on a strength-weight basis it is necessary to reduce the thickness of the individual sheets or sections to the minimum possible value. The fact that the elastic instability of these thin sheets varies inversely as the square of the flat-pitch ratio requires that flat surfaces be broken up by corrugations, ridges, vee grooves and other irregularities. Flat-pitch ratio is defined as the ratio of the width of the widest flat side to the thickness of the material.

The practice of corrugating has led to the development of a large number of different cross-sectional shapes for stiffeners used in stressed-skin construction, and for columns used in truss-type construction. Some attempts have been made to investigate the column properties of such irregular cross-sectional shapes, but without a great deal of success. The hardness and toughness of the material, combined with the fact that it is used in such thin sheets, have presented difficult problems to investigators.

When used as columns either as open sections, such as channels, zees, angles or hat-shaped profiles, or when used as closed sections of irregular cross-sectional shapes, such as are investigated herein, corrosion-resistant steel exhibits the same general traits as the lighter alloys, and is subject to the same general type of failure. However, the limitations accompanying these types of failure for the stainless steel have been subject to much less investigation than for the lighter alloys.

The purpose of this investigation was to determine the fundamental principles underlying the column strength of hollow, thin-walled structural sections of stainless steel, such as are used, or may be used in airplane or similar structures requiring extreme refinement of design in the matter of weight reduction, corrosion resistance and high strength.

SCOPE

The scope of this investigation includes column tests of two closed sections of typical shape made from sheets of nominal thickness 0.006 in., 0.008 in.,

0.010 in., 0.012 in., 0.014 in. The material was 18–8 chrome-nickel, corrosion-resistant steel. It is austenitic at room temperatures. Pin-end as well as flat-end tests were run. Compressive tests were made to determine the elastic properties of the material in compression. The scope was necessarily limited because of the limited number of shapes available for test. Thin stainless steel is not a material which may be readily worked by an amateur with the aid of a few hand tools. It is extremely hard and tough, and may be fabricated successfully only with the aid of special mechanical devices and by experienced workmen.

Although the range of the investigation was limited to closed sections, the technique developed and used is also applicable to the testing of open sections such as mentioned above. Open sections are subject to the same type of failure as closed ones and in addition they may fail by twisting, as has been investigated elsewhere.[1] A few tests were conducted using channels, in order to show that the special technique of preparation and testing could be extended to open sections.

The cross-sectional shapes of the sections investigated are shown in Fig. 1. The section designations S-22 and S-23 are those of Fleetwings, Inc., who furnished the material. The geometrical properties are given in Table 1.

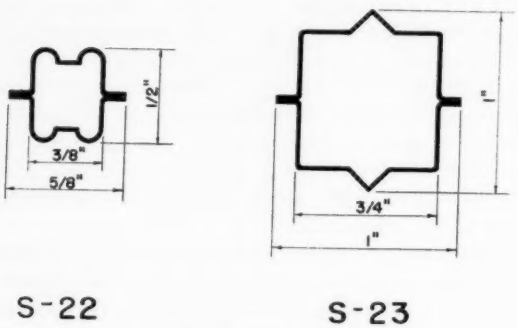

FIG. 1. Stainless steel sections tested.

TABLE 1

Section Properties

Sec.	A	$I\ x\text{-}x$	$I\ y\text{-}y$	$K\ x\text{-}x$	$K\ y\text{-}y$
S-22	$2.228t$	$0.0614t$	$0.0722t$	0.166	0.180
S-23	$3.56t$	$0.3245t$	$0.342t$	0.302	0.310

The areas and moments of inertia were calculated from the centerline dimensions of the sections. The moments of inertia were computed on the assumption that the corners were square, and the areas were computed on the same assumption, except that one thickness of material was deducted for each 90 degree bend. This latter procedure is consistent with shop practice, and the results obtained by it agree with those found by measuring flattened-cut specimens. The sections are fabricated by drawing strips of full-hard, 18–8 corrosion-resistant steel through a set of forming rolls which shape the flat stock into the desired contours. In order to produce closed sections, flanged channels are made. These are then joined at the flanges by a continuous roll-welding process which spaces the welds at any desired interval. The spacing for the sections used was approximately $^3/_{16}$ in. The specimens are uniform in shape and have the minimum possible amount of material along the joined flanges.

The S-22 sections were furnished in nominal gages of 0.006 in., 0.008 in., 0.010 in., 0.012 in. The S-23 sections were furnished in nominal gages of 0.006 in., 0.008 in., 0.010 in., 0.012 in., 0.014 in. The thickness of the actual material differed somewhat from the nominal value and was determined for each specimen by weighing. Owing to the compact shape of the cross-section it was difficult to determine the actual gage by measuring with a micrometer. The density of the material was determined from a piece of flat sheet, and found to be 0.290 lb. per cu.in.

It was not possible to run complete sets of tests on all of the gages listed above, since in some cases the supply of individual thicknesses was limited. This shortage did not hamper the investigation, however, and there are no appreciable gaps because of it.

Prior to the undertaking of any actual column tests it was necessary to make a thorough study of the problems involved in testing and in preparing for test the hard, thin-walled sections which were used. There is very little information on the subject, and that which was found was not applicable to the solution of the problems in hand.

End Finishing

All of the specimens which were tested had flat, parallel ends. The matter of obtaining consistently similar ends within close limits required an improvement in the procedure currently used for this operation. It has been general practice to require that stainless steel column test specimens be finished to within 0.002 in. of being flat and parallel, and the plane of each end be perpendicular to the longitudinal axis of the specimen.[2] The conditions are usually obtained by grinding in a surface grinder. The use of a grinding wheel on the end of a clamped-down specimen is satisfactory in the case of heavy, thick-walled specimens, but is not applicable in the case of material 0.006 in. thick, for example. The thin elements vibrate under the action of the grinding wheel and a wavy surface is produced on the end of the piece. A great improvement in the method of finishing was obtained by grinding the ends of each specimen against an emery cloth disc which was fastened by rubber cement to a steel disc bolted to a lathe face plate. The specimen was held by hand in an angle bracket mounted in the lathe cross carriage. All parts of the apparatus were carefully machine-ground.

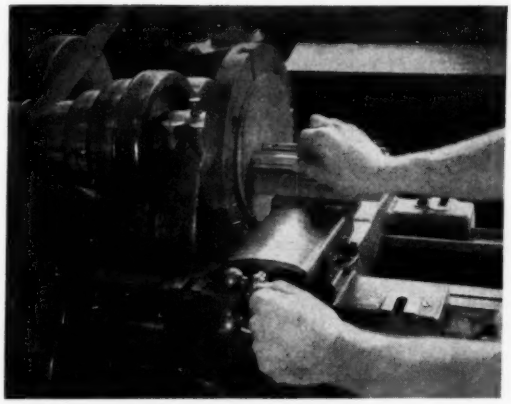

FIG. 2. End finishing apparatus for long specimens.

The angle bracket was carefully set prior to the grinding of any group of specimens. The arrangement shown in Fig. 2 consists of a single disc, and was used for the longer specimens. In finishing any specimen, one hand was used to hold it securely against the angle rest, and at the same time to push it against the emery disc. The other hand cranked the cross carriage of the lathe, carrying the specimen, back and forth across the semi-diameter of the disc in order to wear the disc uniformly. After two or three passes the piece was removed and the burrs taken off by a scraping tool. A finishing grind was accomplished by holding the specimen in the angle bracket as before, but allowing it to rub against the grinding disc only slightly. The cross carriage was again moved laterally in order to assure uniform wear. The piece was then rotated end-for-end about a horizontal axis and the process repeated for the other end. In all cases roughing and finishing cuts were alternated. This resulted in keeping the surface of the wheel true, and permitted the use of one piece of emery cloth for over two hundred specimens. A careful operator can finish both ends of a specimen in about five minutes.

The conditions of flat ends were checked by holding the specimens against a ground and hardened steel block held up to the light. If any light could be seen between the specimens and block, or if there was any tendency to rock, the specimen was refinished. A further check was provided for the short specimens as follows: the flat loading blocks used in the testing machines were carefully located, and shimmed up in order to make them parallel. The short specimens were then inserted in the machine and the heads brought together in order to pinch the piece very lightly. If the specimen had flat, parallel ends normal to its longitudinal axis, it would rub smoothly at both ends when rotated by hand. Any irregularities were indicated instantly by the tendency of the piece to ride or rotate about any high points, or to resist rotating at all in the case of the ends not being parallel.

Owing to the fact that the ends of the sections tend to spring out of shape slightly, it was necessary to devise a two-disc grinding apparatus for the short specimens. When these pieces are flipped end-for-end, any minor distortion results in the production of ends which are not square and parallel after grinding. To correct this defect, a pair of the finishing discs was mounted on a ground shaft, and each disc was carefully and accurately ground. The specimen to be finished is held in a short angle bracket which, in turn, slides in the angle bracket of the original fixture. The use of the parallel grinding wheels removes the necessity of rotating the specimens in order to finish both ends. The arrangement is shown in Fig. 3.

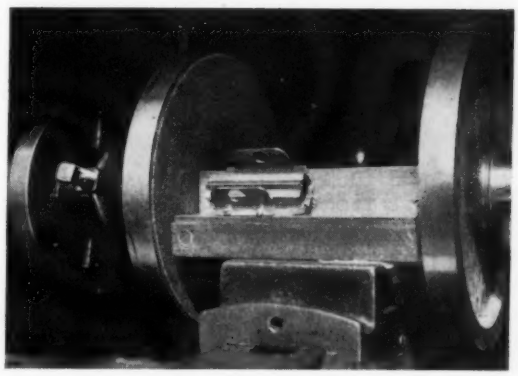

FIG. 3. Two-disc end finishing apparatus for short specimens.

COLUMN TEST DEVICES

Pin-end column tests were conducted by means of a new type of column testing fixture which allows pin-end conditions to be obtained for specimens having flat ends.[3] This is shown in Fig. 4. The original device is made in pairs. Each unit consists essentially of a round, hardened steel bar supported with axis horizontal, between two ball bearing assemblies. The middle portion of the bar has a wide slot milled at its center. The surface of this slot is ground down to a plane which lies exactly in the plane of the diameters of the ball bearing assemblies. The non-Brinell rating of the fixture is 24,000 lbs. and the flexural rigidity of the loading bar is such as to allow an angular deflection of 1.2° under this load. The design play in the bearings allows an angular deflection of 1.5° in the loading bar prior to binding of the bearings. Since maximum test loads were less than 8000 lbs. the fixture had an ample factor of safety against bearing failure or binding.

The preliminary jig just described has many advantages over other devices previously used for the same purpose. It is easy to install and align. The axes of rotation of the ends of the specimens lie in the plane of the loading and thus no correction for effective

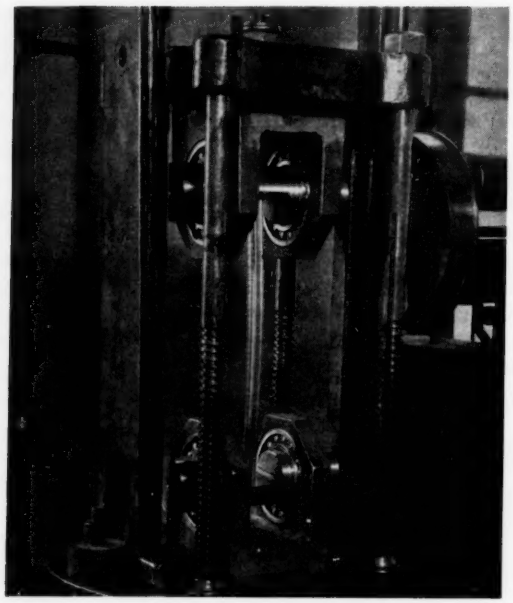

FIG. 4. Pin end column testing fixture (single degree of freedom).

length of the column is required. The loading bars may be statically balanced in the case of delicate tests, and pin-end tests may be run on flat-end specimens.

Extensive use of the fixture[14] indicated that it was quite satisfactory for the use for which it was designed.

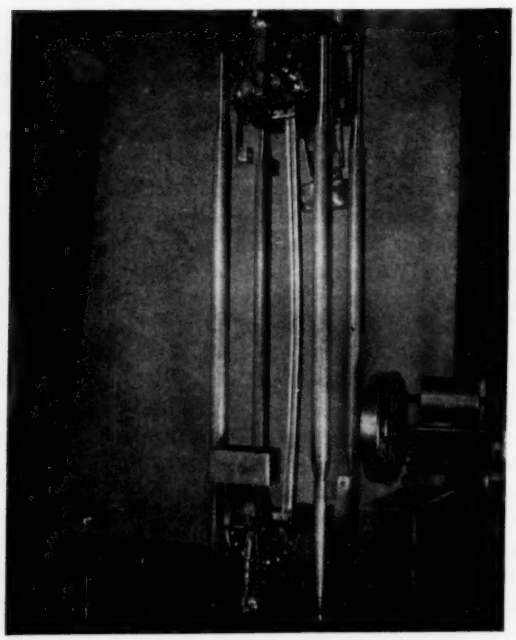

FIG. 5. Pin end column testing fixture (two degrees of freedom).

Furthermore, the scope of its application could be broadened if it were provided with two degrees of freedom, instead of one, and redesigned so as to accommodate specimens having a length less than six inches.

A new jig, shown in Fig. 5, was built. This fixture has two degrees of freedom, uses half bearings, and can be used for the testing of specimens as short as one-half inch. It is counter-weighted in order to be statically balanced about both axes of rotation. Cradling pins are provided in order to prevent the individual units from falling apart during transit, during assembly in the testing machine, or when column failure occurs. The principles employed in this new fixture are basically the same as those used in the simpler one.

Owing to the type of construction employed in the single degree freedom jig, it was not possible to conduct tests to determine the coefficient of friction, although the desirability of doing so was realized. Since the two fixtures were of similar construction it was believed that friction tests on the new type of fixture would be indicative of the results which might be expected from the simpler device. By removing the cradling arms and aligning plates it is possible to bring the two halves of the jig together for the purpose of measuring the coefficient of friction of the assembly. Owing to the extreme freedom of movement of the assembly this proved to be difficult in practice although it sounded well in theory. Since the bearing assemblies used for each axis of freedom were of the same size and type it was felt that a test about one axis would be representative. This test was conducted by assembling the base castings and the accompanying half-bearings around a cylindrical steel bar. The torque required to start rotation of the bar under various compressiye loads on the assembly was determined. The coefficient of friction equals the torque divided by the product of the normal load multiplied by the diameter of ball centers. The effect of the friction is to produce an eccentricity which is equal to the coefficient of friction multiplied by the diameter of the ball centers. The results of the tests indicated that this would amount to an eccentricity of not more than 0.0039 in. at 100 lbs. and 0.00595 in. at 6000 lbs. for the jig having a single degree of freedom. Later experience indicated that these were of negligible magnitude. In addition to these friction tests, two columns of $^1/_2$ in. diameter bars of cold-rolled steel 24 in. long, gave critical loads of 1523 and 1524 lbs., respectively, when tested with the use of the single degree freedom device. On the basis of the accepted value of the modulus of elasticity of 29×10^6 lbs. per sq.in., this would indicate an end-fixity coefficient of 1.0 for the fixture.

From the results of the two types of tests discussed above, it must be concluded that the fixtures described and used in the investigation of the stainless steel columns would provide as close an approach to the ideal value of $C = 1.0$ for pin-end tests as is necessary

for accurate experimental testing and development work.

The pin-end column testing fixture described above represents one of the best devices now in use for testing columns. Notwithstanding the existence of other devices developed for the same purpose, various investigators have preferred to conduct column tests with flat blocks. It has been assumed that flat-end tests develop end-fixity coefficients having values ranging from two to four, and in some instances it has been assumed that the restraint is the same as that developed for continuous members in aircraft structures.

The lack of definite information on the end-fixity produced by flat-end tests seemed to be a good reason to investigate and evaluate it with the aid of the pin-end testing equipment.

A complete series of flat-end column tests was run on both the S-22 and the S-23 sections; these were duplicates of the pin-end tests. Fig. 6 shows a specimen under test.

The column tests were conducted on two different Tinius Olsen, hand-operated, screw-type machines. One was located at New York University and used for testing columns ten inches or less in length, while the other machine was located in the structures laboratory of Fleetwings, Inc., and used for testing the longer columns.

Imbedding Plates

It has been common practice to use imbedding plates between the ends of stainless steel column test specimens and the steel loading blocks of the testing machine. Lead, copper, aluminum, aluminum alloy, wet cardboard, pyralin sheets softened in hot water, and various other compositions have been used. The purpose of the plates is to restrain the ends of the test specimen and thus to avoid failure or distortion at the ends. It has been assumed that this practice would produce a uniform stress distribution over the ends of the specimens.

Several tests with aluminum alloy imbedding plates, as well as without imbedding plates were conducted on duplicate specimens. Flat-end test procedure was used. It was found that there was no local failure at the ends when no plates were used, but that the use of imbedding plates gave unsatisfactory results. In the latter cases the thin outstanding flanges of the specimens resisted imbedding and buckled locally. Furthermore, the results from the tests with imbedding plates were erratic, as compared with those from tests without the imbedding plates. This experience indicated that the use of imbedding plates introduced another cause for failure and was quite unnecessary.

The only satisfactory method for securing even distribution of load is to have the ends finished flat and parallel. Neither imbedding plates nor any other devices will remedy the faults of improperly finished ends.

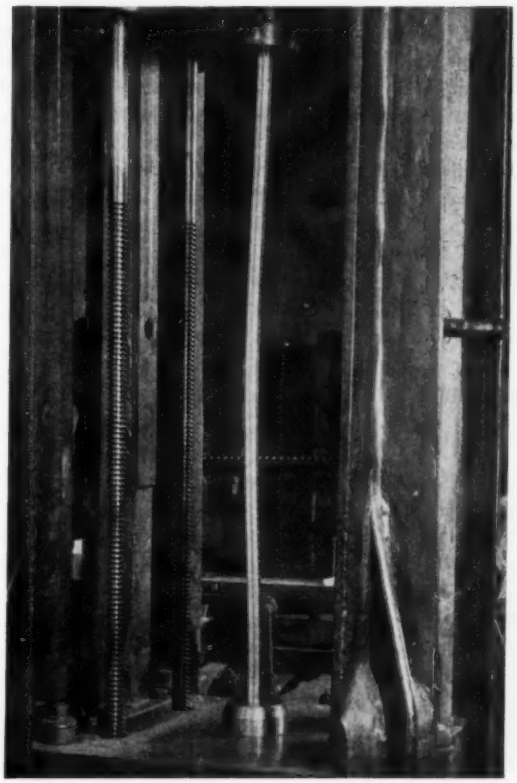

Fig. 6. Typical flat end column text (long column).

Casting the Ends

It has been suggested by some investigators that the ends of the thin metal sections might be cast in small slugs of material such as Wood's metal (melting point about 150°F.). The purpose of this is to provide a restraint for the ends of the specimens and prevent any local distortion. In order to check the value of this procedure, a number of samples of open and of closed sections were prepared with and without cast ends, and flat-end tests were conducted with them. The results of the tests on the closed sections were generally erratic. The results of flat-end tests on a series of $\frac{1}{4}$ in. $\times$ $\frac{1}{2}$ in. $\times$ 0.010 in. channels indicated that the major effect of casting the ends of this section is a shortening of the effective length of the column by an amount equal to the portion of the column encased in the casting. Casting made no difference in the manner of failure. It may be concluded, therefore, that this process is not necessary, and in fact, is likely to indicate a false value of the column strength.

Use of Pre-Stressed Specimens

In some cases it has been the practice to test a piece having a high slenderness ratio and, after failure, to cut two shorter specimens from the apparently undamaged portion of the column. This is done in order

to obtain three different tests from the one long specimen. The impropriety of this as applied to structural steel columns has been noted by Basquin.[5] In order to check the inapplicability of this procedure to the stainless steel testing, several flat-end tests were conducted using these so-called pre-stressed specimens. These had all been cut from longer pieces previously tested. In most cases it was found that the pre-stressed specimens of a given length failed at higher loads than new, unstressed specimens of the same length. As in the case of the specimens tested with imbedding plates, the results from the pre-stressed pieces were generally erratic. The conclusion was confirmed that it was not advisable to use specimens which had been subject to loads in previous tests.

Centering Under Load

Current practice in column testing makes use of centering the compressive specimens under load.[6, 7] The purpose is to account for any irregularities or deviations from straightness of the column, by means of centering the column and adjusting the location of its ends. These are moved until the lateral deflection of the middle of the column is extremely small and does not vary between loads of 150 lbs. and loads representing about 90 per cent of the maximum load expected. The refinement of the column testing process as represented by this method increases the accuracy of the results, but in some cases may be superfluous.

The properties of the stainless steel used in this investigation were such as to preclude the use of this procedure. It is inadvisable to impose any degree of pre-stressing on this material because of its extreme sensitivity to cold working. This response to cold working is generally advantageous, since it increases the strength and elastic properties of the material. However, varying amounts of cold working have varying effects, and the repeated loading to high stresses involved in the process of centering under load would undoubtedly result in a greater scattering of test points than would the small eccentricities obtained in original centering, and the small deviations from straightness. Moreover, Osgood, a proponent of centering under load,[7] says, "If, when the free lengths of the test columns have been computed, plots of average stress at failure against ratio of slenderness based on the computed free length, or modifications of these quantities that take into account the variations in the properties of the material, lie on a reasonably smooth curve, this fact may be regarded as proof that small initial curvatures under conditions of proper centering do not affect the strengths of even inelastic columns freely supported or elastically restrained at the ends." The fact that such consistent results were obtained in this investigation substantiates the soundness of the centering process which was used.

For the flat-end tests this procedure consisted simply of locating the loading blocks approximately in the center of the testing machine heads, and locating the specimen, by eye, in the approximate center of the loading blocks. For the pin-end tests, the loading bars were carefully lined up in the machine so that their axes were in the plane normal to the lower head of the testing machine. The specimens were centered with respect to the bars by a careful procedure which restricted the error to 0.0005 in.

Lateral Movement of Movable Head

Basquin,[5] in his study of tests on structural steel columns, noted that there might be considerable discrepancy due to tilting or shifting of the heads of the testing machine. Means were not available for preventing these motions on the machines used here, but an effort was made to have the specimens centered in the machine. It is not believed that these variables were of much importance in the tests reported in this paper. The test points show such a small tendency to scatter that the effect of unrepeatable factors, such as testing machine head tilting or shifting, must have been negligible.

Test Procedure

As far as possible in view of the supply of the various gages of the two sections, S-22 and S-23, pin-end tests were conducted on specimens having slenderness ratios from 20 to 140, in intervals of ten. A slenderness ratio of 140 for the S-23 section represents a length of 42 in. A duplicate set of specimens having a similar range of slenderness ratios was tested as flat-end columns; in addition, a number of shorter pieces, down to lengths of one inch, were tested as flat-end columns. All loads were applied slowly and evenly. The tests were conducted on hand-operated machines; the beam was always kept balanced, and the critical load determined by the drop of the beam.

Elastic Properties of the Materials

"Plug" method tests were conducted in order to determine the elastic properties of the material in compression.[15] Nominal gages of 0.006 in., 0.008 in., 0.010 in., 0.014 in. were tested for the S-23 sections and of 0.006 in., 0.008 in., 0.010 in., 0.012 in. were tested for the S-22 sections. Huggenberger type "A" tensometers were used to measure strain. Two instruments were used for each test. They were attached near the midpoint of the sections at points near the "outside" corners of the flat sides having the greatest width. Loads were applied slowly and evenly, and frequent readings of strain were made. The movement of the machine head was stopped each time a strain reading was taken, and the indicating hand of the strain gage was allowed to come to rest before reading. The process permitted a condition of equilibrium to be established in the piece.

Duplicate specimens of each gage and section were

tested. In about one-half of the tests the loading process was stopped at a point representing approximately the yield strength of the material, as defined later. At this point the load was allowed to decrease. Strain readings at various loads were taken during this unloading process which was continued until all load had been removed. In the remainder of the tests the load was applied until secondary failure occurred, as indicated by a wrinkling of the free flange or of the widest flat side. The results of the material tests are shown in Fig. 9.

Column Theory

Lundquist proposes a rational classification of column failure which is dependent upon the type of failure which occurs.[1, 5] In this classification, column failures are divided into two groups:

(a) Primary, or general failure, which is defined as any type of failure in which the cross-sections are translated, rotated or both translated and rotated, but not distorted in their own plane.

(b) Secondary, or local failure, which is defined as any type of failure in which cross-sections are distorted in their own plane, but not translated or rotated.

It was found that analysis of the columns investigated herein could be based upon this classification of Lundquist's. The phenomena related to these types of failures are generally well known. For primary failure, the equation for critical stress is:

$$P/A = \frac{c\pi^2 E'}{(L/K)^2} \tag{1}$$

where E' is used to designate the effective modulus of elasticity. It is customary to write this equation as follows:

$$P/A = \frac{\pi^2 E'}{(L'/K)^2} \tag{2}$$

where L' equal $L/\sqrt{c}$.

For cases where the critical stress for primary failure is less than the proportional limit of the material, Eq. (2) is the Euler equation,[9] and E' has the value of E_c, the Young's modulus in compression. For columns where the stress at primary failure exceeds the proportional limit of the material, Euler's formula no longer applies. For such cases the "double modulus" is applicable.[9, 10] The double modulus has a value somewhere between the Young's modulus in compression and the tangent modulus in compression, E_t, at the particular critical stress. The exact value depends upon the material as well as upon the cross-sectional shape of the piece. Templin established that the tangent modulus could be used in place of the double modulus for various aluminum alloys,[11] and Basquin reached the same conclusions after analysis of steel column tests.[5] This procedure also proved to be valid for the sections and materials investigated herein.

Since the end-fixity coefficient, C, for the pin-end tests is known to have a value of 1.0, it was possible to determine the value of the end-fixity coefficient for the flat-end test specimens from the flat-end test results. It was found that in all cases, for both sections and all gages the value of this was four.

Non-Dimensional Coordinates

Whenever column test results are represented by curves wherein average stress is plotted against slenderness ratio there will be some unavoidable scattering of the test points. This variation is due to the variations in the geometry of the individual sections as well as the variations in the material from which they are made. This latter variability can be corrected to the extent to which the stress-strain relations remain invariable along the length in any one given specimen and are affinely related from specimen to specimen.[7] Osgood proposes that the stress-strain relationship be reduced to a non-dimensional relationship,[7] and also proposes that column test results be likewise plotted on non-dimensional coordinates.

Considering this latter suggestion first, it is noted that Osgood proposes the following coordinates:[7]

$$\sigma_s = (P/A)/S \text{ as ordinate, and} \tag{3}$$

$$\lambda_{os} = (1/\pi)(L'/K)\sqrt{S/E_c} \text{ as abscissa} \tag{4}$$

It was suggested in reference 7 that S be determined from the compressive stress-strain diagram of the material in each specimen as the intersection with the stress-strain curve of a line through the origin having a slope βE where β is a constant for a given material, and varies between 0 and 1.0, and E is taken as E_c, the Young's modulus in compression.

The value of S may be chosen also in ways different from that proposed above. In this paper S is taken as the compressive stress at which the material exhibits a shortening under load of 0.002 in. per inch in excess of that which would be computed from a Young's modulus of elasticity, E_c equal to 25×10^6, and the usual formula: $\sigma = E_c \times \epsilon$.

The value of the stress S so obtained corresponds to the definition of yield strength given in Navy Department specification 44, T 27, and is sometimes referred to as proof stress.[7] If this value of S is used, the corresponding value of E_c of 25×10^6 should also be used in the non-dimensional relationship.

In some cases it may be more convenient to select S arbitrarily as a value close to the yield strength of the material (as previously defined). This latter method will generally give satisfactory results provided the value of S so selected does not vary greatly from specimen to specimen and represents a rough mean of the yield strengths. Actually it does not make much difference how S and E are selected, provided E has a value close to the compressive modulus of elasticity of the material at zero stress, E_c, and provided S has a

value approximately equal to the compressive yield strength of the material.

The advantage of plotting on the non-dimensional coordinates is that all column test data or all stress-strain data, whichever is being plotted, will fall on one and the same curve, provided the various original stress-strain curves of the material are affinely related.

It follows as a logical conclusion that these individual curves, one developed from the material test results and the other developed from the column test results, will be identical provided the proper values of the variables and the constants are selected. It is necessary, of course, that the same system of non-dimensional coordinates be used for plotting column test results as well as material test results.

In reducing the column test results for primary failure to the non-dimensional system, reference is made to Eq. (3), where P/A should be taken as the critical average unit stress at which primary failure occurs.

In order to reduce the material test data to the non-dimensional system, Eq. (4) must be modified in such a manner that it will include the compressive elastic properties of the material. If the value of (L'/K), as obtained from Eq. (2), is substituted in Eq. (4) the following relationship is obtained:

$$\lambda'_{os} = (1/\pi)(\pi)\sqrt{\frac{(E')}{(P/A)} \times \frac{(S)}{(E_c)}} = \sqrt{\frac{E'}{P/A} \times \frac{S}{E_c}} \quad (5)$$

In order to correlate column test data with material test data, it is necessary to select the proper value of the effective modulus E', which when substituted in Eq. (5) and used with Eq. (3) will produce a curve identical to that produced from the use of Eqs. (3) and (4). This value of E' is obviously the value which satisfies Eq. (2), which is the general formula representing critical stress for primary column failure. In accordance with the currently accepted theory, E' represents the double modulus, $\overline{E}$, which for some materials and sections, including those investigated herein, may be in turn represented by the tangent modulus in compression, E_t.

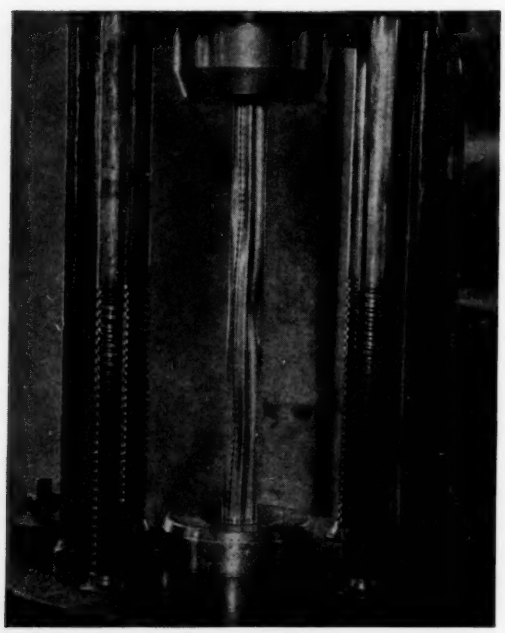

FIG. 7. Type of secondary failure—Sec. S-23.

SECONDARY FAILURE

For the analysis of secondary failure Timoshenko's methods may be applied.[9] The phenomenon of secondary failure of sections having flat elements depends upon the elastic stability of the individual elements composing the section, as well as upon the degree of edge support furnished to each element by all or any of the other elements of the section.

The critical stress for secondary failure is defined as the average unit stress over the whole cross-section existing when any element of the section becomes elastically unstable. If the load is increased after secondary failure occurs, the stress distribution over the section will no longer be uniform and with further increase in load additional elements will fail until the entire section collapses. This progressive failure is probably some function of the effective slenderness ratios of the various elements of the cross-section.

The critical stress for elastic stability of a flat plate subject to end compression and having various degrees of support along the edges is given as:

$$f_{cr.} = \frac{k\pi^2 t^2 E_c}{12(1 - \mu^2)b^2} \quad (6)$$

This equation as written applies only to stresses below the proportional limit of the material. It appears logical to apply it to conditions existing beyond the proportional limit by substituting the effective modulus in compression E', for Young's modulus E_c. The equation is then:

$$f_{cr.} = \frac{k\pi^2 t^2 E'}{12(1 - \mu^2)b^2} \quad (7)$$

For sheets having a large ratio of length to width, k is a factor dependent only on the degree of restraint or elastic support provided at the edges of the sheet.

For the purpose of analyzing entire sections of complex shape by investigation of the stability of the flat sides, the term k as used by Timoshenko for the simpler cases of flat sheets having various degrees of support along the edges may be replaced by a particular value R. This R is defined as an effectiveness factor. It represents the effectiveness of the restraint and support provided at the edges of the element which fails first. It applies only in the cases where the length of the flat element is several times its width.

It was determined in this investigation that R is sub-

stantially constant for a given geometrical section and invariant with thickness of material.

The value of R may be determined from the crinkling tests of a few short specimens. From results of such tests and by means of Eq. (7), R is found from the following expression:

$$R = \frac{(P/A)12(1 - \mu^2)b^2}{\pi^2 E' t^2} \tag{8}$$

The maximum slenderness ratio at which secondary failure is critical may be determined by equating the critical stresses for primary and secondary failure Eqs. (2) and (7) wherein R is substituted for k in Eq. (7), then,

$$f_{cr.} = \frac{\pi^2 E'}{(L'/K)^2} = \frac{R\pi^2 E' t^2}{12(1 - \mu^2)b^2}$$

from which:

$$L'/K_{cr.} = \frac{b}{t}\sqrt{\frac{12(1 - \mu^2)}{R}} \tag{9}$$

Typical forms of secondary failure are shown in Figs. 7 and 8.

Test Results

Data from the compressive stress-strain tests of the fabricated sections as shown in Fig. 9 were reduced, by using Eqs. (3) and (5), to the non-dimensional basis previously referred to. Results of the calculations are plotted in Fig. 11 and a faired curve is drawn through the points.

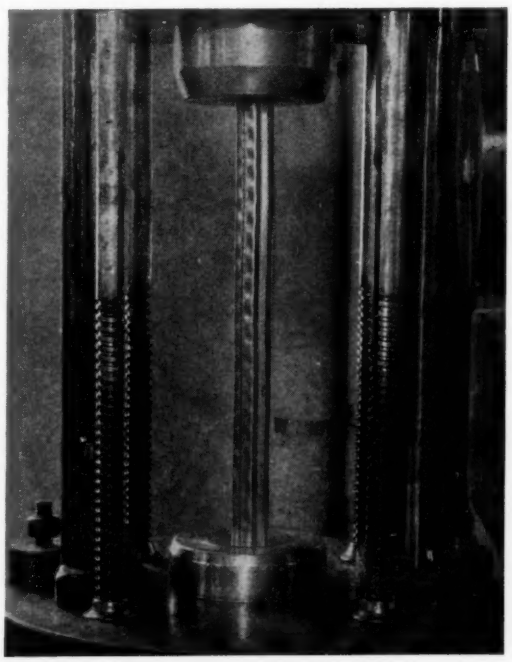

Fig. 8. Type of secondary failure—Sec. S-23.

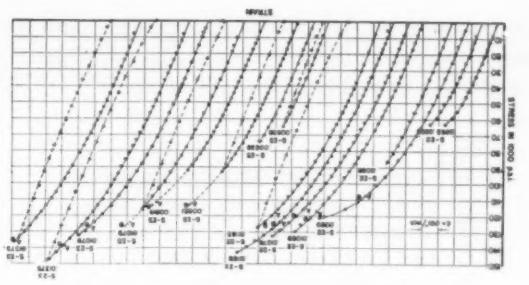

Fig. 9. Compressive stress-strain curves.

Typical results of column tests are shown on Fig. 10 where average unit stress is plotted against slenderness ratio. Data from tests of the other section and the other gages gave similar results. Flat-end tests have been reduced to equivalent pin-end lengths on the assumption that C for flat-end tests is 4.0. The curve drawn on Fig. 10 represents Eq. (2) wherein the tangent modulus in compression E_t, as obtained by the "Plug" method, is used for the effective modulus E'. The agreement of the results of column tests with the curve so drawn is a first substantiation that the tangent modulus in compression so obtained satisfies the equation for primary failure of the columns tested in this investigation. No attempt has been made to analyze the type of failure that occurred after secondary failure took place. The horizontal line on Fig. 10 represents the value of the average unit stress at secondary failure as obtained by the use of Eq. (9). This will be discussed later.

The results of column tests on all gages of both sections have been reduced to the non-dimensional values represented by Eqs. (3) and (4), where the values of S and E_c for each gage and section are the same as those obtained in the tests of reference 15. Flat-end test results are reduced to pin-end test results on the basis of $C = 4.0$ for flat-ends. The test points representing column test results are plotted on Fig. 12. The curve drawn on this figure is identical with that of Fig. 11.

Values of σ_s, representing secondary failure in accordance with Eq. (9), are shown as horizontal lines on Fig. 12. The value of b as used in this equation is

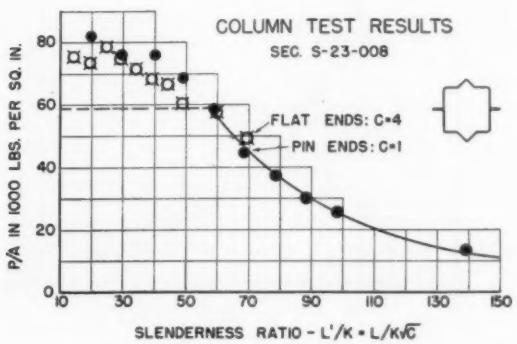

Fig. 10. Typical result of column tests.

the width of the flat side which fails first. This width is measured from midpoint to midpoint of the adjacent supporting flanges (or the point of tangency of large radii, as for the S-22 section). The value of μ was assumed to be constant and equal to 0.30. The factor R was evaluated from tests of short columns and determined to be as follows:

Sec. S-22	$R = 3.60$
Sec. S-23	$R = 6.90$

Critical values of slenderness ratio, L'/K, expressed by Eq. (9), were found for the nominal gages of the two sections. These, in turn, were substituted in the dimensional and non-dimensional equations for column strength and plotted on the diagrams which show the column test results. In order to prevent confusion in the regions of the curves representing low values of λ_{os}, many of the points representing tests of very short columns were omitted. There were so many of these that any plotting of them would only obscure the important test points.

There is presented in Table 2 a summary and comparison of critical stresses for secondary failure as determined from four different sources, as follows:

1. From the column curves, such as shown on Fig. 10, where P/A is plotted *versus* L'/K. The critical stress for secondary failure may be obtained by using the critical value of L'/K from Eq. (9) in conjunction with the column curve.

2. From the non-dimensional curves which are drawn using particular values of S obtained from the compressive stress-strain curves for the particular section and gage. The critical stress for secondary failure is found from Fig. 12. σ_s and λ_{os} are obtained by the use of Eqs. (3) and (4). The value of L'/K used in Eq. (4) is the value obtained from Eq. (9).

3. From the non-dimensional curves which were drawn using an arbitrary value of S equal to 125,000 lbs. per sq.in.[15] The critical stress for secondary failure is then found in the manner given for item (2) above.

4. From the results of a few tests of short columns.

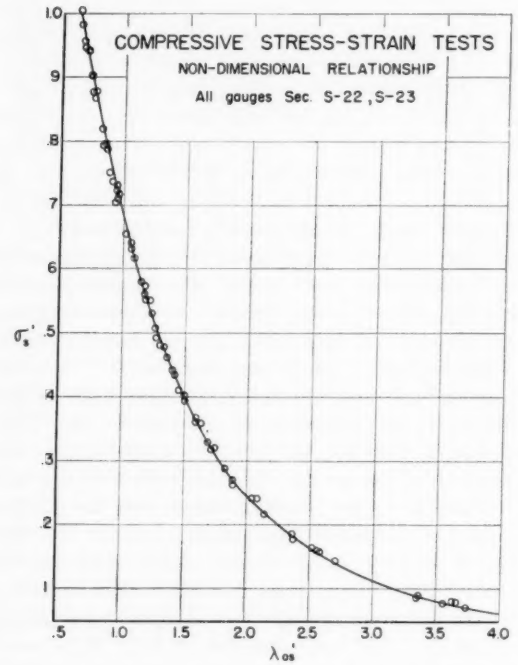

FIG. 11. Plug method stress-strain relationships plotted to non-dimensional system of coordinates.

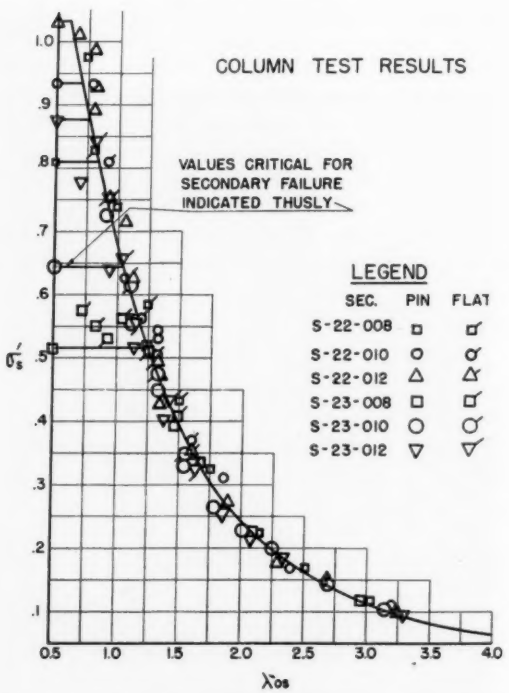

FIG. 12. Column Test results plotted to non-dimensional system of coordinates.

CONCLUSIONS

1. An inexpensive and rapid method has been developed for preparing flat-end specimens of thin-walled stainless steel for column test.

2. A fixture having a single degree of freedom of rotation has been developed for obtaining pin-end conditions in column testing. This device permits accurate reduction of column data and gives consistent results as judged from the close correlation obtained with material test data. A modification of this fixture has been developed which will permit obtaining two degrees of freedom. Both fixtures permit the use of flat-end specimens and require no correction for effective length.

3. Evidence indicates that the use of imbedding plates in column testing is unnecessary, provided the ends of the specimens have been accurately finished

TABLE 2

Summary and Comparison of Critical Stress Values for Secondary Failure

Sec.	σ_1 ÷ 1000	σ_2 ÷ 1000	σ_3 ÷ 1000	σ_4	R—Calc. from Test	Act. Ga. from Test
S-22-006	59.0		66.8			
008	92.5	88.2	93.7			
010	113.0	114.0	114.0			
012	127.0	129.1	127.5			
S-23-006			37.6	>44.0	>7.15	0.00641
				<52.8	<9.2	0.00641
				≈37.8	≈6.75	0.00597
008	59.0	58.3	60.0	>56.2	>6.30	0.00801
				<63.5	<8.04	0.00801
010	81.5	81.7	80			
014	121.0	120.6	121.5	≈117.4	≈6.80	0.01369

flat and parallel. The use of imbedding plates is likely to produce premature secondary failure.

4. The use of pre-stressed specimens gives unsatisfactory results, and there is little justification for using material which has been subject to prior test.

5. There is no need to cast the ends of column test specimens in Wood's metal or other material in order to prevent secondary failure at the ends of the specimens. Adequate care in finishing the ends of the specimens has no substitute.

6. The "Plug" method has been developed for use in determining the compressive stress-strain relationship for thin-walled sections. It is especially applicable to built-up or other fabricated sections of material for which the elastic properties may have been altered by cold working or other processing.

7. Carefully conducted column tests with flat-end specimens on flat, parallel loading blocks will develop end-fixity coefficients C, of 4.0.

8. Thin-walled closed sections of 18–8 stainless steel, of the type investigated herein, develop primary failure (becomes elastically unstable as a whole) at stresses indicated by Eq. (2), where E', the effective modulus of elasticity, is represented by the tangent modulus of elasticity E_t. This tangent modulus must be determined from compressive stress-strain tests on the fabricated sections, particularly if the material is such that the elastic properties are affected by cold working or other processing incident to forming.

9. Secondary failure of the above type of specimens occurs at a critical effective slenderness ratio expressed by Eq. (9), in which R is a section constant for any given geometrical shape, and is invariant with the thickness of the sheet.

10. Results of column tests on sections such as are investigated herein may be successfully represented on plots using non-dimensional coordinates whose values are expressed in Eqs. (3) and (4). The results of these tests when so plotted show good correlation with the results of compressive stress-strain tests when the latter are similarly reduced to the same basis with the aid of Eqs. (3) and (5). The compressive tangent modulus should be used to represent the effective modulus in all of the expressions for primary failure.

REFERENCES

[1] Lundquist, E. E., *On the Strength of Columns that Fail by Twisting*, Journal of the Aeronautical Sciences, Vol. 4, No. 6, April, 1937.

[2] Matulaitis, J., and Schwartz, E. H., *An Investigation of the Compressive Properties of Stainless Steel Sheet-Stringer Combinations*, Part IV, U.S. Army Air Corps. Information Circular, Vol. 8, No. 708, February, 1937.

[3] Barlow, H. W., *A Fixture for Obtaining Pin-End Conditions in Column Testing*, Journal of the Aeronautical Sciences, Vol. 7, No. 2, December, 1939.

[4] Aitchison, C. S., and Tuckerman, L. B., *The "Pack" Method for Compressive Tests of Thin Specimens of Materials Used in Thin-Walled Structures*, N.A.C.A. Technical Report No. 649, 1939.

[5] Basquin, O. H., *Tangent Modulus and the Strength of Steel Columns in Tests*, Technological Paper No. 263, U.S. Bureau of Standards, September, 1924.

[6] Osgood, W., and Holt, M., *The Column Strength of Two Extruded Aluminum Alloy H. Sections*, N.A.C.A. Technical Report No. 656, 1939.

[7] Osgood, W., *Column Strength of Tubes Elastically Restrained Against Rotation at the Ends*, N.A.C.A. Technical Report No. 615, 1938.

[8] Lundquist, E. E., *Local Instability of Centrally Loaded Columns of Channel Section and Z Section*, N.A.C.A. Technical Report No. 722, 1939.

[9] Timoshenko, S., *Theory of Elastic Stability*, McGraw-Hill, New York, 1936.

[10] Osgood, W. R., *The Double Modulus Theory of Column Action*, Civil Engineering, Vol. 5, No. 3, pages 173–175, March, 1935.

[11] Templin, R. L., Sturm, R. G., Hartman, E. C., and Holt, M., *Column Strength of Various Aluminum Alloys*, Tech. Paper No. 1, Aluminum Research Laboratories, Aluminum Company of America, Pittsburgh, Pa., 1938.

[12] Lundquist, E. E., *Local Instability of Symmetrical Rectangular Tubes under Axial Compression*, N.A.C.A. Technical Note No. 686, 1939.

[13] Osgood, W. R., *Column Curves and Stress-Strain Diagrams*, Bureau of Standards Journal of Research, Vol. 9, No. 492, October, 1932.

[14] Propper, E. M., *The Column Strength of Certain Thin-Walled Stainless Steel Sections*, A thesis, Guggenheim School of Aeronautics, New York University, 1939.

[15] Barlow, Howard W., Lu, Ho-Shen, and Stillwell, Henry S., *The "Plug" Method for Obtaining the Compressive Elastic Properties of Thin-Walled Sections*, Journal of the Aeronautical Sciences, Vol. 8, No. 3, January, 1941.

Shear Center of a Multi-Cell Metal Wing

H. W. SIBERT

University of Cincinnati

SUMMARY

Simple formulas based on the least work of shear are given for the coordinates of the shear center and the shear force per unit length of arc of a multi-cell wing beam. The terms involved in these formulas are ordinary summations or can be evaluated by Simpson's Rule according as concentrated areas or skin effective in bending is concerned. A numerical example is worked out for the case of a two-cell wing beam with skin on the tension side effective in bending.

INTRODUCTION AND NOMENCLATURE

THE GENERAL principles for obtaining the shear center of a multi-cell metal wing by means of the least work of shear have been given by Hatcher.[1] Due to the complexity of the analysis only single-cell beams, such as leading-edge wing beams, have been treated so far.[1, 2, 3, 4] The purpose of this paper is to extend the methods developed in references 2 and 4 to metal wings containing two or more cells. Since the effect of taper on shear center is apparently small for modern metal wings,[3] the analysis will be limited to a wing of uniform cross-section.

The following symbols and sign conventions will be used in this paper:

C_c = cross-section for which shear center is desired

S = variable point on the skin of C_c

s = distance along the skin of C_c from a starting point to point S (always +)

q_S = shear flow, or shear force/unit length of skin, at S (+ when in direction of arrows shown in Fig. 2)

I = moment of inertia of entire cross-section C_c with respect to the principal axis about which the beam is bending

L, t = length and thickness of a segment of the skin of C_c

$K_{MN} = \int_M^N ds/t = \sum L/t$ for segment MN (always +)

Q_{MN} = statical moment about a principal axis of that part of the skin of C_c between points M and N which is effective in bending

$J_{MN} = \int_M^N Q_{MS} ds/t = \int_M^N Q_{MS} dK_{MS}$, M and N being points

P = a fixed point on web ca of C_c between points c and a (Fig. 2)

A_{MN} = area bounded by the portion of the skin of C_c between points M and N and by the radial lines PM and PN (always +)

$\beta_{MN} = \int_M^N Q_{MS}\, dA_{MS}$, M and N being points

a_i = area of a concentrated area whose center of gravity is at a point i

M_P = moment about P of the shear flow in the entire cross-section C_c (+ when counterclockwise)

D_P = distance from P to the shear center measured parallel to the principal axis about which the beam is bending; $D = M_P/F$

$\sum_{SR} Y_i$ = $Y_0 + Y_n + 4\sum Y_i$ (odd i's) $+ 2\sum Y_i$ (even i's), which is the summation in Simpson's Rule when Y is the integrand of the integral to be evaluated and the interval between the limits of integration is divided into n (even) equal parts

Subscripts 1, 2, 3 when applied to K, Q, and A refer to the closed circuits *abca*, *acdea* and *dfged*, respectively, of Fig. 2.

FUNDAMENTAL FORMULAS

For constant cross-section and constant shear modulus the work of shear in the wing between C_c and the loaded cross-section is[4]

$$W = (B/2G) \int q_S^2\, ds/t \qquad (1)$$

where G is the shear modulus and B is the spanwise distance from C_c to the loaded cross-section.

Fig. 1 shows a portion of the beam of spanwise length dx with C_c the face at distance x from some origin. With the shear flow in C_c as shown in Fig. 1, the summation of forces in the x direction gives $q_1\, dx + q_2\, dx = q_3 dx + q_4 dx + dP$, where P is the resultant of the bending forces on the portion of C_c shown in Fig. 1. Let F

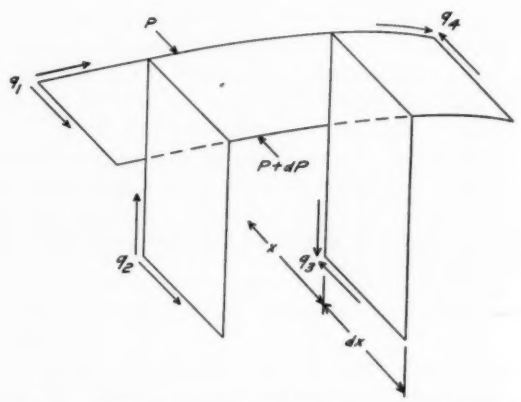

FIG. 1. Relation between shear flow and bending forces.

Received October 21, 1940.

be the component of total shear force on C_c perpendicular to the principal axis about which the beam is bending and let F be positive when in the positive direction of the other principal axis. Then, $dP/dx = FQ/I$, where Q is the statical moment of the portion of C_c shown in Fig. 1. Hence, $q_1 + q_2 = q_3 + q_4 + FQ/I$. Note that q_1 and q_2 can be thought of as flowing into, and q_3 and q_4 as flowing out of, the portion of C_c shown in Fig. 1. Then, for the particular case of $F = 1$, the last relation connecting q_1, q_2, q_3, and q_4 can be written

$$\sum q \text{ (in)} = \sum q \text{ (out)} + (1/I)\sum Q \text{ (interior)} \quad (2)$$

Since q (in) and q (out) act along the cuts which bound the sub-section of C_c, Eq. (2) is also valid when the sub-section of C_c contains a closed contour of the skin. Thus, Eq. (2) is valid for all sub-sections of C_c, provided that $F = 1$.

In reference 4 it was shown that the contribution of a segment MN of C_c to the moment M_P about a fixed point P equals the integral of $(2q_S\, dA_{MS})$ from M to N. Thus, M_P is the summation of these integrals taken over all the segments of C_c. When Eq. (2) is used to find q_S, $D_P = M_P$ because $D_P = M_P/F$ and Eq. (2) was obtained by taking $F = 1$. Hence, when q_S is found from Eq. (2),

$$D_P/2 = M_P/2 = \sum(\textstyle\int_M^N q_S\, dA_{MS}) \quad (3)$$

in which the summation is taken over all segments MN with each term positive or negative according as the moment of the shear flow in that segment is counterclockwise or clockwise, because M_P itself is positive when counterclockwise.

Let x and y be the principal axes of C_c and let x point to the right and y point upward. Since $D_P = M_P/F$, D_P is positive when both M_P and F are positive, that is, when M_P is counterclockwise and F is up for bending about the x axis or to the right for bending about the y axis. Hence, a positive D_P in Eq. (3) requires the shear center to be to the right of the y axis or below the x axis according as there is bending about the x or y axes.

Three-Cell Wing

The three-cell beam in Fig. 2 is triply indeterminate so far as shear flows are concerned, and the shear flow q_S at any point can be obtained only after the shear flow at one point in each of the three cells has been found. Let the three shear flows to be determined be q_c, q_c' and q_d at infinitesimal distances to the left of point c, to the right of c, and to the right of point d, respectively (Fig. 2). By means of Eq. (2) and suitable sub-sections of the beam it can be shown that q_S has the following values:

$$\left.\begin{aligned} q_S &= q_c - Q_{cS}/I \text{ on } cba \\ q_S &= q_c - q_c' + Q_{cS}/I \text{ on } ca \\ q_S &= q_c' + Q_{cS}/I \text{ on } cd \\ q_S &= q_c' - q_d + Q_{cdS}/I \text{ on } de \\ q_S &= q_d + Q_{dS}/I \text{ on } dfge \\ q_S &= q_c' - (Q_1 + Q_{aS})/I \text{ on } ae \end{aligned}\right\} \quad (4)$$

The three least-work conditions, $\partial W/\partial q_c = 0$, $\partial W/\partial q_c' = 0$ and $\partial W/\partial q_d = 0$ can now be applied to Eq. (1). By virtue of Eq. (4) and the definitions of K and J these three conditions yield, respectively,

$$K_1 q_c - K_{ac} q_c' = (J_{cba} - J_{ca})/I \quad (5)$$

$$K_2 q_c' - K_{ac} q_c - K_{de} q_d = (Q_1 K_{ae} + J_{ca} + J_{ae} - J_{cde})/I \quad (6)$$

$$K_3 q_d - K_{de} q_c' = (Q_{cd} K_{de} + J_{de} - J_{dfge})/I \quad (7)$$

the term $Q_{cd}K_{de}$ in Eq. (7) being due to the breaking up of Q_{cdS} on segment de into $Q_{cd} + Q_{dS}$. Note that q_c, q_c', and q_d can be obtained by solving Eqs. (5), (6), and (7) simultaneously.

From Eqs. (3) and (4) and the definitions of A and β,

$$D_P/2 = A_1 q_c + A_2 q_c' + A_3 q_d + (\beta_{cde} + \beta_{dfge} - \beta_{cba} - \beta_{ae} - Q_1 A_{ae})/I \quad (8)$$

because with point P on ca the moment of the shear flow in ca about point P is zero and $A_{cba} = A_1$, $A_{cd} + A_{de} + A_{ae} = A_2$ and $A_{dfge} - A_{de} = A_3$. Eq. (8) gives the correct sign of D_P because the values of q_S in Eq. (4) were based on the directions of shear flow shown in Fig. 2 and these directions all give a counterclockwise moment about point P when P is on ca.

All the formulas necessary for locating the shear center of a three-cell beam have now been given. A similar analysis will solve an n-celled wing ($n > 3$). For such a wing there will be n simultaneous linear equations connecting the n unknown shear flows, q_c, q_c', q_d .... in the n cells.

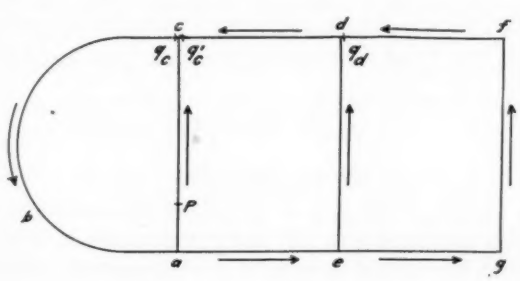

Fig. 2. Three-cell wing.

Two-Cell Wing

Let the two-cell wing be the wing in Fig. 2 with section $dfge$ cut off. The effect of removing section $dfge$ is to eliminate entirely Eq. (7), which came from $\partial W/\partial q_b = 0$, and to delete from Eqs. (4), (5), (6), and (8) all terms containing q_b or pertaining to section $dfge$. The final results are:

$$K_1 q_c - K_{ac} q_c' = (J_{cba} - J_{ca})/I \tag{9}$$

$$K_2 q_c' - K_{ac} q_c = (Q_1 K_{ae} + J_{ca} + J_{ae} - J_{cde})/I \tag{10}$$

$$D_P/2 = A_1 q_c + A_2 q_c' + (\beta_{cde} - \beta_{cba} - \beta_{ae} - Q_1 A_{ae})/I \tag{11}$$

After q_c and q_c' have been found from Eqs. (9) and (10), D_P can be obtained from Eq. (11).

An alternative form for Eqs. (10) and (11) can be derived from the first two formulas of Eq. (4) and the relation $q_S = q_c' + Q_{cS}/I$ on $cdea$. Then, the two least-work conditions, $\partial W/\partial q_c = 0$ and $\partial W/\partial q_{c'} = 0$, applied to Eqs. (1) and (3) change the right-hand side of Eq. (10) to $(J_{ca} - J_{cdea})/I$ and the last term of Eq. (11) to $(\beta_{cdea} - \beta_{cba})/I$. By means of the relations $Q_1 + Q_{cdea} = 0$, $J_{MN} + J_{NM} = Q_{MN} K_{MN}$ and $\beta_{MN} + \beta_{NM} = Q_{MN} A_{MN}$ in conjunction with Eq. (17) and the corresponding equation for β_{BCDE} these alternative forms of Eqs. (10) and (11) can be transformed into the original forms.

By definition the first power only of Q is involved in J and β. Moreover, the Q for the skin alone is zero for any portion of the skin not effective in bending. Hence, the total Q, J or β for any segment of C_c equals the sum of the Q, J or β of the concentrated areas associated with the segment plus the Q, J or β of that portion of the skin of the segment which is effective in bending.

Skin Effective in Bending

In reference 4 formulas have been given for J and β for a segment of the skin of constant thickness when it is effective in bending. If MN is such a segment and if the segment is divided into n (even) equal parts with the points of division numbered from 0 to n beginning with point M and ending with point N, the β, J and Q for bending about the x axis are:

$$\beta_{MN} = L_{MN} t_{MN} (\textstyle\sum_{SR} A_{Ni} y_i)/3n \tag{12}$$

$$J_{MN} = \{C_{n-2} + 2C_{n-4} + 3C_{n-6} + \ldots + (n/2)C_0\} 4L^2_{MN}/3n^2 \tag{13}$$

$$Q_{MN} = L_{MN} t_{MN} (\textstyle\sum_{SR} y_i)/3n = (C_0 + C_2 + C_4 + \ldots + C_n) 2L_{MN} t_{MN}/3n \tag{14}$$

where

$$\left.\begin{aligned} C_0 &= y_1 + y_0/2,\ C_n = y_{n-1} + y_n/2 \\ C_i &= y_{i-1} + y_i + y_{i+1},\ i \neq 0 \text{ or } n \end{aligned}\right\} \tag{15}$$

If a J (or β) refers to a segment comprising two or more sub-segments, this J (or β) can be reduced to the sum of the J's (or β's) on the sub-segments plus certain quantities involving Q. This is accomplished by letting the Q on each sub-segment equal the sum of the Q's on the previous sub-segments plus the Q on the segment in question; for example, Q_{BCS} on sub-segment CD of a segment BCD equals $Q_{BC} + Q_{CS}$. By virtue of such relations and the definitions of K and J it can be proved that

$$J_{BCD} = J_{BC} + J_{CD} + Q_{BC} K_{CD} \tag{16}$$

$$J_{BCDE} = J_{BCD} + J_{DE} + Q_{BCD} K_{DE} \tag{17}$$

The corresponding formulas for β_{BCD} and β_{BCDE} are obtained by replacing each J and K in Eqs. (16) and (17) by β and A, respectively. By means of these relations the problem of finding any J or β in Eqs. (5) through (11) reduces to that of finding the J or β on segments of constant thickness, to which Eqs. (12) and (13) are applicable. Note that when Q is zero at every point of a segment, J is also zero for that segment. Thus, $J_{BCD} = J_{CD}$ in Eq. (16) if $Q = 0$ at every point of sub-segment BC.

In applying Eqs. (12) through (15) to a section MN of corrugated skin of constant thickness, the y's can be measured to the median line of the corrugations, but L_{MN} must be the developed length of the corrugated skin instead of the length of its median line.

Concentrated Areas

It is customary to assume that the area of each longitudinal stiffener is concentrated at its center of gravity, the area of each stiffener on the compression side being augmented by the effective area of the skin associated with it. The work of shear stresses in such concentrated areas is so small that it is usually neglected, the entire work of shear occurring in the skin of the outer perimeter and shear webs. These concentrated areas, however, do have an appreciable effect on the work of shear, because the transference to the skin of the effect of the statical moment of each concentrated area causes a change in the shear flow in the skin. Since the shear load in a stiffener is transmitted to the skin through its connecting rivets, the effect on the skin of the statical moment of each concentrated area, so far as shear flow in the skin is concerned, can be assumed to be concentrated at a point on the skin coinciding with the center line of a single row of connecting rivets or midway between the center lines of a double row of connecting rivets.

When concentrated areas only are involved, it is convenient to consider each concentrated area separately in the integral defining J (or β), the total J (or β) being the sum of these individual integrals. Thus, for the concentrated areas associated with a segment MN of skin, the J and β for bending about the x principal axis are:

$$J_{MN} = \textstyle\sum a_i\, y_i\, K_{i'N} \tag{18}$$

$$\beta_{MN} = \Sigma a_i\, y_i\, A_{i'N} \tag{19}$$

in which a_i is the area of any one of the concentrated areas associated with MN and i' is the point on MN to which the statical moment of a_i is transferred. When the Q for a concentrated area is transferred to the skin

at the junction point M of two adjacent segments HM and MN, it can be associated with either HM or MN but not with both of them.

Straight-Line Segment of Constant Thickness

Let MN be a straight-line segment of the skin of constant thickness t_{MN}, and let δ_{MN} be the perpendicular distance from point P to line MN. If S is a point on MN and ds is the differential of arc along MN, $dA_{MS} = \delta_{MN}\, ds/2$. Then, from the definitions of β, J and A,

$$\beta_{MN} = \int_M^N Q_{MS}\, \delta_{MN}\, ds/2 = \delta_{MN}\, t_{MN}\, J_{MN}/2 \quad (20)$$

$$A_{MN} = \delta_{MN}\, L_{MN}/2 = \delta_{MN}\, t_{MN}\, K_{MN}/2 \quad (21)$$

Note that Eqs. (2) and (21) are valid for concentrated areas as well as for skin effective in bending.

For skin effective in bending, the substitution of any even integer for n in Eqs. (13) and (12) yield, respectively,

$$J_{MN} = (2y_M + y_N)\, L^2_{MN}/6 \quad (22)$$

$$\beta_{MN} = (2y_M + y_N)\, L_{MN}\, t_{MN}\, A_{MN}/6 \quad (23)$$

The J_{MN} and β_{MN} for the concentrated areas associated with segment MN can be obtained from Eqs. (18) and (19).

Neutral Axis

If the skin is thin, the skin on the tension side of a cross-section is entirely effective in bending while on the compression side only the effective width of skin associated with each longitudinal stiffener is effective in bending. For this reason, the section properties of a cross-section cannot be determined until the location of the neutral axis (the line separating the tension and compression sides of the cross-section) is known. In general, the angle between the neutral axis and any orthogonal set of axes, u and v, through the center of gravity of the cross-section is a function of the section properties of the cross-section with respect to u and v and the components of the resultant moment about the u and v axes. Formulas for determining this angle are given in reference 3. Although the neutral axis of an airplane wing coincides with the beam principal axis (the one nearly perpendicular to the beam forces on the wing) only when the resultant shear force is actually parallel to the beam direction, the angle between the neutral axis and the beam principal axis is usually very small. Hence, it is generally accurate enough to assume that the neutral axis coincides with the beam principal axis when calculating the section properties of a wing cross-section.

Axes Not Principal Ones

Let R_x or R_y stand for any one of the parentheses on the right side of Eqs. (5) through (11) according as there is bending about the x or y principal axes. Let x' and y' be any other pair of axes through the center of gravity of C_c, let θ be the angle (+ when counterclockwise) from the positive x' axis to the positive x axis and let $R_{x'}$ and $R_{y'}$ be the same functions of y' and x', respectively, as R_x is of y. Since R_x contains the first power of y only, R_y, $R_{x'}$ and $R_{y'}$ contain the first power only of x, y' and x', respectively. Moreover, since $x = y' \sin\theta + x' \cos\theta$ and $y = y' \cos\theta - x' \sin\theta$,

$$R_y = R_{x'} \sin\theta + R_{y'} \cos\theta \quad (24)$$

$$R_x = R_{x'} \cos\theta - R_{y'} \sin\theta \quad (25)$$

$$I_y = (I_{x'} + I_{y'})/2 + H_{x'y'}/\sin 2\theta \quad (26)$$

$$I_x = (I_{x'} + I_{y'})/2 - H_{x'y'}/\sin 2\theta \quad (27)$$

$$\tan 2\theta = 2H_{x'y'}/(I_{y'} - I_{x'}) \quad (28)$$

in which H stands for product of inertia. If one prefers, the values of R_x, R_y, I_x and I_y required in Eqs. (5) through (11) can be obtained directly from the x' and y' axes by means of Eqs. (24) through (27) without first having to find the coordinates of any point of the beam with respect to the x and y axes (the principal axes).

Example

The cross-section shown in Fig. 3 will be taken as an example. The nose is a circle of 4-inch radius, but all other segments of the skin are straight lines. Segments ca and de are each 0.02 inch thick while segment $dcbae$ is 0.03 inch thick. Only the portion of the skin below

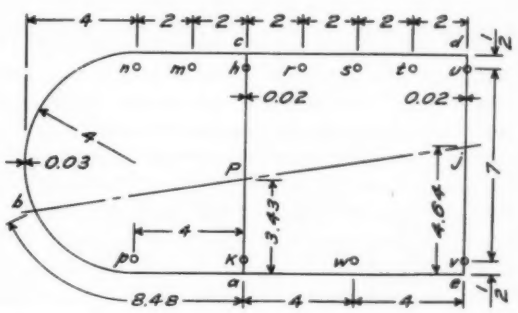

Fig. 3. Two-cell wing used in the example.

the neutral axis (the tension side) will be assumed to be fully effective in bending. The 7 upper concentrated areas, n, m, h, r, s, t and u each contain 0.12 sq.in., including the effective area of the associated skin. The 4 lower concentrated areas, p, k, w and v, each contain 0.1 sq.in. exclusive of any portion of the skin. It will be assumed that the Q of each concentrated area is transferred to the skin as follows: areas h, k, u and v to webs ca and de at points coinciding with their respective centers of gravity; areas n, m, r, s and t to segment dc and dc extended at points directly opposite their respective centers of gravity; areas p and w to segment ea and ea extended at points directly opposite their respective

centers of gravity. By the usual methods, the center of gravity of Fig. 3 was located 0.36 inch below and 1.37 inch to the right of the midpoint of line *ca* and the *x* principal axis (*bj* in Fig. 3) was rotated 8° 32′ counterclockwise from line *ae*. It will be assumed that *bj* is also the neutral axis of Fig. 3 and that point *P* is at the intersection of lines *bj* and *ca*. Table 1 gives the data for finding J and β for the concentrated areas, the last

TABLE 1

Concentrated Areas

Concentrated Areas			Segment of Skin				
Name	a	y	Name	K	A	ayK	ayA
h	0.12	4.02	ha	375	0	180.90	0
k	0.1	−2.90	ka	25	0	− 7.25	0
			ca			173.65	0
m	0.12	4.32	$m'ba$	618.88	52.56	320.83	27.25
n	0.12	4.62	$n'ba$	552.21	47.99	306.15	26.61
p	0.1	−2.30	$p'a$	133.33	6.86	− 30.67	− 1.58
			cba			596.31	52.28
r	0.12	3.73	$r'de$	600	45.71	268.56	20.46
s	0.12	3.43	$s'de$	1600/3	41.14	219.52	16.93
t	0.12	3.14	$t'de$	1400/3	36.57	175.84	13.78
u	0.12	2.84	ue	375	30.00	127.80	10.22
v	0.1	−4.09	ve	25	2.00	− 10.22	− 0.82
			cde			781.50	60.57
w	0.1	−3.50	$w'e$	400/3	6.86	− 46.67	− 2.40
			ae			− 46.67	− 2.40

two columns listing the quantities appearing in Eqs. (18) and (19). Table 2 gives data needed for Q, J and β of segment *ba* of the skin when *ba* is divided into 6

TABLE 2

Segment *ba* of Skin

Point	y	c_i	$(3-i/2)c_i$	A_{ai}	$A_{ai}y_i$
0 (b)	0	−1.26	−3.78	19.50	0
1	−1.26			14.60	−18.40
2	−2.22	−6.23	−12.46	10.50	−23.31
3	−2.75			7.30	−20.08
4	−2.97	−8.90	−8.90	4.87	−14.46
5	−3.18			2.44	− 7.76
6 (a)	−3.39	−4.875		0	0
Totals		−21.265	−25.14		
Σ_{SR}					−260.50

equal parts, the third, fourth and sixth columns listing quantities which appear in Eqs. (14), (13) and (12), respectively. Hence, for concentrated areas only (see Table 1):

$$J_{ca} = 173.65,\ J_{cba} = 596.31,\ J_{cdc} = 781.50,$$
$$J_{ae} = -46.67,\ \beta_{cba} = 52.28,\ \beta_{cde} = 60.57,$$
$$\beta_{ae} = -2.40,\ Q_1 = 0.12(4.02 + 4.32 + 4.62) + 0.1(-2.9 - 2.3) = 1.0352$$

For skin alone (see Table 2 and Fig. 3):

$L_{ba} = 8.48,\ L_{Pa} = 3.43,\ L_{je} = 4.64,\ L_{ae} = 8$
$y_a = -3.39,\ y_e = -4.59,\ \delta_{ae} = 3.43,\ \delta_{je} = 8$
$J_{ba} = -25.14 \times 8.48^2/27 = -66.96$ (Eq. (13))
$\beta_{ba} = -260.5 \times 8.48 \times 0.03/18 = -3.68$ (Eq. (12))
$Q_{ba} = -21.265 \times 8.48 \times 0.03/9 = -0.6011$ (Eq. (14)
$J_{Pa} = (2 \times 0 - 3.39)3.43^2/6 = -6.65$ (Eq. (22))
$Q_{Pa} = 0.02 \times 3.43\ (-3.39)/2 = -0.1163$
$J_{je} = (2 \times 0 - 4.59)4.64^2/6 = -16.47$ (Eq. (22))
$\beta_{je} = 8 \times 0.02\ (-16.47)/2 = -1.32$ (Eq. (20))
$J_{ae} = \{2(-3.39) - 4.59\}8^2/6 = -121.28$ (Eq. (22)
$\beta_{ae} = 3.43 \times 0.03\ (-121.28)/2 = -6.24$ (Eq. (20))

For skin and concentrated areas:

$J_{ca} = 173.65 - 6.65 = 167.00$
$J_{cba} = 596.31 - 66.96 = 529.35$
$\beta_{cba} = 52.28 - 3.68 = 48.60$
$J_{cde} = 781.50 - 16.47 = 765.03$
$\beta_{cde} = 60.57 - 1.32 = 59.25$
$J_{ae} = -46.67 - 121.28 = -167.95$
$\beta_{ae} = -2.40 - 6.24 = -8.64$
$Q_1 = 1.0352 - 0.6011 - 0.1163 = 0.3178$
$Q_1K_{ae} = 0.3178 \times 8/0.03 = 84.75$
$Q_1A_{ae} = 0.3178 \times 3.43 \times 8/2 = 4.36$
$K_{ac} = 8/0.02 = 400,\ K_1 = 8/0.02 + (8 + 4\pi)/0.03 = 1085.55$
$K_2 = (8 + 8)/0.02 + (8 + 8)/0.03 = 1333.33$
$A_1 = 4 \times 8 + 8\pi = 57.13,\ A_2 = 8 \times 8 = 64$
$I_x = 22.66$
$1085.55q_c - 400q_c' = (529.35 - 167)/22.66 = 15.99$ (Eq. (9))
$1333.33q_c' - 400q_c = (84.75 + 167 - 167.95 - 765.03)/22.66 = -30.06$ (Eq. (10))
$q_c = 0.00722,\ q_c' = -0.02038$
$D_P/2 = 57.13(0.00722) + 64(-0.02038) + (59.25 - 48.6 + 8.64 - 4.36)/22.66$ (Eq. (11))
$D_P = -0.47$ inch (to left of P)

The D_P for bending about the y axis is found by a similar process with I_y replacing I_x and x replacing y in the formulas for Q, J and β. An actual airplane wing would not be much more difficult than this example, the only added complication being that *ae* would be a curved line and would require an additional table similar to Table 2 for the calculation of its J and β.

REFERENCES

[1] Hatcher, Robert S., *Rational Shear Analysis of Box Girders*, Journal of the Aeronautical Sciences, Vol. 4, No. 6, page 233–238, April, 1937.

[2] Sibert, H. W., *Shear Distribution in a Sheet-Metal Box Spar*, Journal of the Aeronautical Sciences, Vol. 5, No. 4, page 134–137, February, 1938.

[3] Newell, Joseph S., *The Analysis of Leading-Edge Wing Beams*, S.A.E. Journal, Vol. 45, No. 3, page 385–388, September, 1939.

[4] Sibert, H. W., *Shear Center of a Leading-Edge Wing Beam*, Journal of the Aeronautical Sciences, Vol. 7, No. 12, page 520–523, October, 1940.

Propulsive Effects of Radiator and Exhaust Ducting

MANFRED RAUSCHER, *Massachusetts Institute of Technology*
AND
W. H. PHILLIPS, *National Advisory Committee for Aeronautics*

SUMMARY

It is shown how the thrust and the thermal efficiency of a ducted radiator vary with the design of the duct, the amount of radiator heating and the airplane speed. The type of duct commonly used for drag reduction is found to serve well for thrust recovery. Nevertheless, the thermal efficiency of the arrangement is so low that the thrust obtainable is unlikely to offset more than about one-third of the drag of the radiator and duct.

A study is made of the thrust given by a jet of fluid released in a duct. Conditions are found to exist under which the thrust of the ducted jet is greater than that of the jet unducted. If the jet consists of cool fluid, the thrust augmentation is secured by a venturi-shaped duct. With a hot jet, an expanding-contracting duct is required, as for a propulsive radiator. The analysis suggests that the potential benefits of exhaust ducting are of the same order as those of radiator ducting.

INTRODUCTION

THE power delivered by a moving engine can be increased through a utilization of the cooling air and the exhaust gases as propulsive jets.

That a propulsive effect should be obtainable from the *cooling air* was suggested several years ago by Meredith.[1] Since then, various writers[2–4] have elaborated on the idea and clarified the basis of its working. The cardinal point is that the expansion of a stream of fluid under heating will result in a speeding up of the fluid, and hence in a propulsive reaction, only if the stream is confined between properly shaped boundaries. The variation of the propulsive effect with the character of these boundaries is examined from an elementary theoretical viewpoint in Part I of this paper.

The possibility of deriving a thrust from the *exhaust gases* by merely pointing the exhaust stacks backward has long been recognized. The propulsive force that can be secured in this way is, however, relatively small.[6] A greater force could, in principle, be produced through a diffusion of the kinetic energy of the exhaust jets into a larger mass of fluid. This has led to the proposal of *thrust augmentors* in the form of various types of ducts around the exhaust stacks.[7–11] An elementary theory of the performance of such devices is developed in Part II of the paper.

PART I
RADIATOR PROPULSION

Radiators in Ducts

The cooling of aircraft engines requires a dissipation of heat into the atmospheric air. The bodies through which this dissipation takes place are termed radiators. If the engine is air-cooled, the engine itself is the radiator. When the engine is cooled by liquid, most of the heat is disposed of through a radiator set apart from the engine. In either case, the radiator is customarily enclosed in a cowling or duct that provides an expanding air channel in front of the radiator and a contracting channel behind the radiator. The primary purpose of these fairings is to keep down the drag by guiding the air through and past the radiator with a minimum of disturbance. As it happens, however, the same type of fairing is capable of extracting propulsive energy from the cooling air. The net drag reduction achieved by a fairing thus varies with the extent to which this propulsive effect is utilized.

Thermodynamics of Propulsive Action of Ducted Radiators

The derivation of a propulsive effect from the heating of a ducted stream can be explained in terms of simple thermodynamics if the fluid is a gas, like the air in the problem under study:

While slowing down and gaining pressure in its motion through the entrance section of the duct, the air compresses essentially adiabatically. Then heat is added at approximately constant pressure as the air passes through the radiator core. Next, the air undergoes essentially adiabatic expansion as it speeds up and loses pressure in the exit section of the duct; and finally it is cooled at atmospheric pressure until it returns to the condition of the entering air. Through this thermodynamic cycle, heat energy is changed into mechanical energy with an efficiency $\eta = 1 - (1/r)^{k-1}$, if r signifies the "compression ratio" of the cycle (*i.e.*, the ratio of the density of the air at the radiator to the density of atmospheric air), and k is the ratio between the specific heats of the cooling air at constant pressure and at constant volume.

If the process is viewed from a system *fixed in the radiator*, so that the air moves while its constraints are stationary, any work absorbed by the air must ultimately appear as an addition to the air's kinetic energy, and so result in an increase in the momentum of the ducted stream. The creation of these energy and momentum changes requires a backward push on the air by the radiator and the duct. The air, in turn, reacts on the radiator and duct with an equal propulsive force.

Received November 27, 1940.

To determine the useful work accomplished, it is necessary to examine this process from a system *fixed in the atmosphere.* The radiator then advances at the velocity of the airplane, while the cooling air stirs relatively little. Most of the work done by the mutual forces between radiator and air thus is done on the radiator, and is therefore utilized for propulsion. The work not utilized is found in the final kinetic energy of the cooling stream relative to still air. To arrive at the propulsive efficiency of the process, it is thus necessary to multiply the thermal efficiency by a factor analogous to the Froude efficiency of a propeller.

Because of the uncertain value of this *Froude factor,* and the inaccuracy of the assumption that the heating of the air takes place at constant pressure, the foregoing analysis does not yield precise results. A number of general conclusions can, however, be drawn from it. For example, the efficiency of the radiator as a propelling device is seen to increase rapidly with the airplane speed, because the compression of the duct air, which determines the thermal part of the efficiency, varies as the square of the speed. The compression depends also on the ratio of the area of the radiator core to the entrance area of the duct. The maximum effect would be secured if this ratio were infinite, so that the flow would reach its full stagnation pressure at the core. An effect almost as great results, however, if the core area is but three or four times the entrance area, as in ducts actually used in practice. A parallel-sided duct would have no compressive effect and would therefore have zero efficiency. This is in line with the observation that no pressure forces could be exerted on the walls of such a duct in the direction of the motion. A venturi-shaped duct would have a negative efficiency, and so would produce a drag under heating.

A rough estimate of the magnitude of the propulsive effect of a well-ducted radiator may be made by assuming that the full stagnation pressure is realized at the radiator core, and that the kinetic energy losses are negligible. Excessive as such an estimate is, it indicates propulsive efficiencies of only a few per cent at the highest airplane velocities yet reached. The power obtainable by radiator ducting thus is unlikely to be more than a small fraction of the propulsive power of the engine itself.

Hydrodynamic View of Propulsive Effect of Radiator Ducting

The thermodynamic process discussed in the preceding Section is but one phase of the energy transformations taking place in the ducted flow. In a broader view of the problem, thermodynamics merges into fluid dynamics and is covered by the latter. Because of the smallness of the density variations in the flow at ordinary speeds, the flow is essentially as it would be in the total absence of compressibility effects. With allowance for a density change brought about by the heating, the problem can thus be treated as one in hydrodynamics.

The cross-sectional area A, velocity v and pressure p of the cooling stream at stations far ahead of the radiator, immediately in front of the core, immediately in back of the core, and far behind the radiator will be marked by the indices shown in Fig. 1. With ρ_1 the density of the unheated fluid, and ρ_2 the density of the heated fluid, Bernoulli's equation applied in front the radiator and behind the radiator furnishes the relations

$$^1/_2\rho_1 v_1^2 + p_1 = {}^1/_2\rho_1 v_2^2 + p_2 \tag{1}$$

and

$$^1/_2\rho_2 v_3^2 + p_3 = {}^1/_2\rho_2 v_4^2 + p_4 \tag{2}$$

Continuity requirements make

$$\rho_1 A_1 v_1 = \rho_1 A_2 v_2 = \rho_2 A_2 v_3 = \rho_2 A_3 v_4 \tag{3}$$

The momentum equation for the flow through the core is

$$(p_2 - p_3)A_2 = \rho_1 v_2 A_2 (v_3 - v_2) \tag{4}$$

and for the thrust T

$$T = \rho_1 A_2 v_2 (v_4 - v_1) \tag{5}$$

From these seven equations, it is possible to determine seven of the variables in terms of the remaining variables. If the former are taken as p_2, v_2, p_3, v_3, A_3, v_4 and T, the solution for T proceeds through the equations

$$T = \rho_1 A_1 v_1^2 \left(\frac{\rho_1 A_1}{\rho_2 A_3} - 1 \right) \tag{6}$$

and

$$\frac{A_1}{A_3} = \sqrt{\frac{\rho_2}{\rho_1}\left[1 + \left(\frac{A_1}{A_2}\right)^2\right] - \left(\frac{A_1}{A_2}\right)^2} \tag{7}$$

to

$$T = \rho_1 A_1 v_1^2 \left\{ \sqrt{\frac{\rho_1}{\rho_2}\left[1 + \left(\frac{A_1}{A_2}\right)^2\right] - \left(\frac{\rho_1 A_1}{\rho_2 A_2}\right)^2} - 1 \right\} \tag{8}$$

Of the variables entering into this expression, ρ_1 and v_1 are given directly. ρ_2 is determined by the temperature rise allowed in the cooling stream. This temperature rise, in conjunction with the specified rate of heat dissipation, fixes the mass flow $\rho_1 A_1 v_1$ through the radiator, and so determines A_1. From the mass flow and the heat dissipation, it is finally possible to determine A_2 for any given type of radiator core.

The quantity $T/\rho_1 A_1 v_1^2$, representing a thrust coefficient based on the initial area and velocity of the cooling stream, is plotted in Fig. 1. The curves show that a positive thrust is obtained only when the ratio A_1/A_2 lies below a critical value which is always less than unity and decreases as the heating increases. For any given amount of heating, the thrust is greatest when A_1/A_2 equals zero, *i.e.*, when the radiator core area becomes infinite. This result agrees with the conclusion reached in the thermodynamic analysis before.

Thrust Calculation Based on Exit Area of Duct

If the duct extended far enough forward and backward, and approached constant cross-sections toward both ends, the cooling fluid would enter the duct at the undisturbed velocity v_1, and the cross-sectional area of the mouth of the duct would be A_1—assuming that the areas of mouth and exit were in the ratio A_1/A_3 called for by Eq. (7). The various quantities entering into the thrust equation could then be computed directly from the layout of the duct. The problem is, however, complicated by the fact that the proper ratio A_1/A_3 varies with the ratio ρ_2/ρ_1, and hence with the heating. Because of this fact, the entrance and exit openings of a fixed duct can be in the correct ratio only under one heating condition. When the ratio between the duct openings is incorrect, the proper ratio A_1/A_3 must establish itself through changes in the cross-section of the cooling stream beyond the ends of the duct. The identification of the entrance opening with A_1 and of the exit opening with A_3 is then no longer permissible.

For a rigorous determination of the actual areas A_1 and A_3 under these circumstances, it would be necessary to resort to experiment. An approximate rational method of obtaining the areas can, however, be based on the known fact that the fluid in a jet emanating from a parallel-sided pipe is roughly at the pressure of the fluid surrounding the jet. This fact suggests that the flow through a duct with a parallel-sided end section will always be such as to yield a discharge jet of nearly constant cross-sectional area. A_3 may, accordingly, be taken to equal the exit area of the duct, while A_1 is left to assume whatever value it must have to satisfy Eq. (7).

Through this argument, the details of the entrance section become irrelevant—so long as the section is wide enough to permit an adequate inflow. To do away with the restriction to a parallel-ended exit section, it is necessary to discover how the ultimate cross-sectional area of a contracting or expanding jet is related to the jet area at a point of given convergence or divergence. Some light on this question can be obtained from studies of propeller slipstreams.[5] The indications are that ducts with walls converging or diverging toward the exit at angles up to 10 or 15 degrees will yield jets whose ultimate cross-sectional area differs from the exit area by but a few per cent. A_3 may thus be taken to equal the exit area of the duct when the duct end is tapered, as well as when it has parallel sides.

The area A_1, in terms of which the thrust was expressed by Eq. (8), is related to A_3 through Eq. (7). Solved for the ratio A_1/A_2 instead of A_1/A_3, the latter equation gives

$$\frac{A_1}{A_2} = \frac{1}{\sqrt{\frac{\rho_1}{\rho_2}\left[1 + \left(\frac{A_2}{A_3}\right)^2\right] - 1}} \tag{9}$$

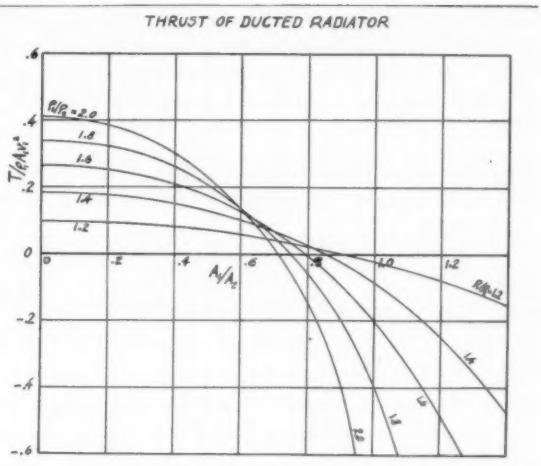

FIG. 1. Dependence of radiator thrust coefficient $T/\rho_1 A_1 v_1^2$ on ratios ρ_1/ρ_2 and A_1/A_2.

The thrust equation can therefore be written explicitly in terms of A_3 as

$$T = \rho_1 A_3 v_1^2 \left\{ \frac{\frac{\rho_1}{\rho_2}}{\frac{\rho_1}{\rho_2}\left[1 + \left(\frac{A_3}{A_2}\right)^2\right] - \left(\frac{A_3}{A_2}\right)^2} - \frac{1}{\sqrt{\frac{\rho_1}{\rho_2}\left[1 + \left(\frac{A_3}{A_2}\right)^2\right] - \left(\frac{A_3}{A_2}\right)^2}} \right\} \tag{10}$$

For the ratio ρ_1/ρ_2, it is possible to write

$$\frac{\rho_1}{\rho_2} = 1 + \tau(\Delta t) \tag{11}$$

with τ the coefficient of thermal expansion of the cooling air at essentially constant pressure, and Δt the difference between the temperatures of the heated and unheated air. This temperature difference is determined by the equation

$$\frac{H}{778} = 32.2\ \rho_1 A_1\ v_1 c(\Delta t) \tag{12}$$

in which H is the rate of dissipation of heat energy, in foot-pounds per second, and c is the specific heat of the cooling fluid, in B.t.u. per pound per degree Fahrenheit. The equation for ρ_1/ρ_2 can thus be written

$$\frac{\rho_1}{\rho_2} = 1 + \frac{H\tau}{(32.2)(778)\rho_1 A_1 v_1 c} \tag{13}$$

or, with $\tau/(32.2)(778)\ c$ lumped into a constant K,

$$\frac{\rho_1}{\rho_2} = 1 + \frac{H}{K\rho_1 A_1 v_1} = 1 + \frac{H}{K\rho_1 A_3 v_1} \cdot \frac{A_3}{A_2} \cdot \frac{A_2}{A_1}$$

$$= 1 + \frac{H}{K\rho_1 A_3 v_1} \sqrt{\frac{\rho_1}{\rho_2}\left[1 + \left(\frac{A_3}{A_2}\right)^2\right] - \left(\frac{A_3}{A_2}\right)^2} \tag{14}$$

or, after transposition, squaring and reduction,

$$\frac{\rho_1}{\rho_2} = 1 + 2\frac{H}{2K\rho_1 A_1 v_1}\left(\frac{H}{2K\rho_1 A_1 v_1}\left[1+\left(\frac{A_3}{A_2}\right)^2\right] + \sqrt{1+\left\{\frac{H}{2K\rho_1 A_1 v_1}\left[1+\left(\frac{A_3}{A_2}\right)^2\right]\right\}^2}\right) \quad (15)$$

This expression, through Eq. (10), now yields the thrust directly in terms of the independent variables ρ_1, v_1, A_2, A_3, H and K.

The dissipation of the heat energy H enables the radiator and duct to do the useful work Tv_1. The arrangement may therefore be said to have an efficiency $\eta = Tv_1/H$. Thus, with the values of T and H given by Eqs. (10) and (14),

$$\eta = \frac{{v_1}^2}{K}\left(\frac{\frac{\rho_1}{\rho_2} - \sqrt{\frac{\rho_1}{\rho_2}\left[1+\left(\frac{A_3}{A_2}\right)^2\right] - \left(\frac{A_3}{A_2}\right)^2}}{\left[\frac{\rho_1}{\rho_2}-1\right]\sqrt{\frac{\rho_1}{\rho_2}\left[1+\left(\frac{A_3}{A_2}\right)^2\right] - \left(\frac{A_3}{A_2}\right)^2}}\right) \quad (16)$$

For given ratios ρ_1/ρ_2 and A_3/A_2, the efficiency is seen to be proportional to the square of the velocity v_1. This result is in agreement with the conclusions reached through the thermodynamic analysis before. The plot of Eq. (16) in Fig. 2 also confirms the expectation that the efficiency would be greatest with an infinite core area, but that the efficiency is only slightly less

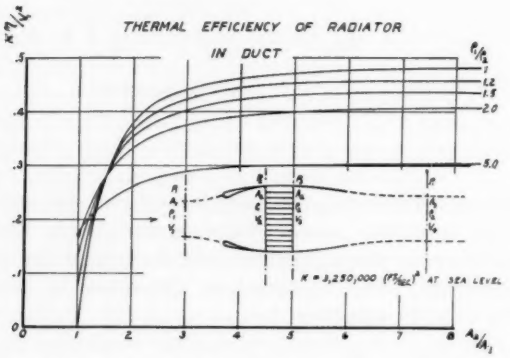

FIG. 2. Variation of thermal efficiency of ducted radiator with ratios ρ_1/ρ_2 and A_2/A_3.

with core areas equal to three or four times the duct openings.

The heat power dissipated by the radiator of a gasoline engine normally equals about 50 per cent of the engine's indicated power, while the propeller delivers in useful form about 75 per cent of this indicated power. The ratio of the energy dissipated through the radiator to the useful work done by the propeller is therefore about $^2/_3$. Multiplication of this ratio by the thermal efficiency of the radiator gives the ratio of the propulsive power of the radiator to the thrust power of the propeller, or, what is the same thing, the ratio of the radiator thrust T to the propeller thrust T_p. Fig. 3, based on the assumption that $c = {}^1/_4$ and $\tau = {}^1/_{520}$, so that $K =$ 3,250,000, shows the relation between T and T_p for a typical case ($\rho_1/\rho_2 = 1.2$, $A_2/A_3 = 4$).

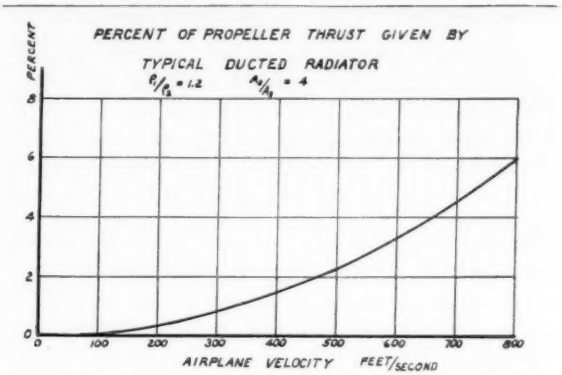

FIG. 3. Relation between thrust of ducted radiator and thrust of propeller at different airspeeds.

Effects of Friction Losses in Radiator and Duct

The assumption of an ideal flow in the foregoing analysis helps to bring out the working essentials of radiator propulsion, but leaves the solution of the problem incomplete, especially through the neglect of the friction loss across the radiator core. To allow for this loss, it is necessary to add a quantity $A_2\Delta p_0$ to the right-hand side of Eq. (4). The thrust equation (8) then becomes

$$T = \rho_1 A_1 {v_1}^2\left\{\sqrt{\frac{\rho_1}{\rho_2}\left[1+\left(\frac{A_1}{A_2}\right)^2 - \frac{\Delta p_0}{{}^1/_2\rho_1 {v_1}^2}\right] - \left(\frac{\rho_1 A_1}{\rho_2 A_2}\right)^2} - 1\right\} \quad (17)$$

Because the ratios ρ_1/ρ_2, A_1/A_2 and $\Delta p_0/{}^1/_2\rho_1 {v_1}^2$ all influence each other in a manner peculiar to each case, a quantitative discussion of this modified thrust equation will not be attempted here. Qualitatively, it is evident that the presence of the term $\Delta p_0/{}^1/_2\rho_1 {v_1}^2$ reduces the radical in the expression, and hence cuts down the thrust. As this radical represents the quantity $\rho_1 A_1/\rho_2 A_3$, it appears also that the exit area of the duct must be increased if the values of ρ_1, ρ_2 and A_1 are to be the same as before, *i.e.*, if the cooling capacity of an actual system is to come up to that of a frictionless one. The whole analysis presumes, of course, that the effective core area is not reduced through flow separation in the entrance section.

Besides the friction loss in the radiator itself, there is also a loss from the air resistance of the duct. Experimental indications are that the combined losses always overbalance the gain to be had from the heating. For density ratios up to 1.2, for example, as found in conventional installations, Fig. 1 shows a thrust coefficient of less than 0.10, while the drag coefficient of a typical unheated radiator and duct system is about 0.30 when based on the same area and velocity. By raising the density ratio to a higher

figure, it would be possible to secure a higher thrust coefficient. This gain would, however, be largely offset by the increased friction losses resulting from the greater viscosity of the hotter air and from the extra cooling surface needed to make up for the reduced temperature difference between the radiator and the air. A thrust somewhat above one-third of the gross drag of the warm radiator and duct thus seems the best that may be expected on the basis of present knowledge.

Part II

Exhaust Propulsion

Ducted Jets

The kinetic energy $mv^2/2$ of a mass m with a velocity v is connected with the momentum mv through the identities

$$mv^2/2 = (mv)(v/2) = (mv)^2/2m$$

The momentum corresponding to a given kinetic energy thus is relatively great when the energy is distributed through a large mass moving slowly, and the momentum is relatively small when the energy is concentrated in a little mass moving fast. It is then possible, in theory, to secure an increase of momentum without expenditure of kinetic energy through a dissemination of the energy into a larger mass.

This theoretical possibility proves difficult to realize in practice. Merely mixing a high speed jet with slower moving fluid in an open stream, for example, yields no benefit, because so much energy is lost in the transfer from jet to fluid that the increased mass with the residual energy has only just the same momentum as the original jet. That no momentum change could be produced by this kind of mixing follows, of course, directly from the absence of any external agent capable of furnishing the force necessary for such a change. The problem of thrust augmentation thus is the dual one of reducing the mixing losses and of providing a support for an accelerating force. This dual requirement can be satisfied by a non-parallel-sided duct around the jet.

Hydrodynamic Theory of Ducted Jets

In the ordinary exhaust collector, which also serves as a muffler, the exhaust gases are slowed down well below the velocity of sound. Compressibility effects are therefore of secondary magnitude, and the flow may be studied by the hydrodynamic method already used in connection with the radiator problem.

The setup considered is shown in Fig. 4. Exhaust gas with a density ρ_e and velocity v_e is assumed to be discharged into a duct from a parallel-walled pipe of cross-sectional area A_e. In accordance with the principle noted in the study of radiator jets, the gas is assumed to emerge from the pipe at the pressure p_2 existing in the duct around the mouth of the pipe. The outer stream has a density ρ_1 and a velocity v_1 far ahead of the duct. The portion of the stream passing through the duct has a cross-sectional A_1 far ahead, and a net area A_2 about the mouth of the inner pipe, past which this ducted flow has a velocity v_2. Mixture of the exhaust gas and of the augmentor fluid finally yields a jet of density ρ_3, cross-sectional area A_4 and velocity v_4 at the open stream pressure p_1 far downstream from the duct.

The mixing of two flows in a channel of variable cross-section is a process that cannot be treated by elementary methods. In the present analysis, it is therefore assumed that the mixing takes place in a parallel-sided section of the duct. Since the duct walls then can exert no axial force on the fluid in this mixing section, the momentum changes occurring in the section are determined by the pressures, densities and velocities at the ends of the section. The effects of the mixing can, accordingly, be allowed for in the same general manner as the effects of the heating in a radiator core.

The results obtained through the assumption of a cylindrical mixing section hold equally when the mixing takes place in an infinitesimal length of a duct of variable cross-section. Such instantaneous mixing could be approximated in practice by the use of a large number of jets instead of one central jet. When the mixing process extends over a distance in which the duct section varies perceptibly, as it usually does under actual conditions, the theory does not apply with rigor. It should, however, still remain a fair approximation so long as the gases are uniformly mixed by the time they finally leave the duct.

Bernoulli's equation applied in front of the mixing section and behind the mixing section gives the relations

$$^1/_2\rho_1 v_1^2 + p_1 = {}^1/_2\rho_1 v_2^2 + p_2 \tag{18}$$

and

$$^1/_2\rho_3 v_3^2 + p_3 = {}^1/_2\rho_3 v_4^2 + p_1 \tag{19}$$

while continuity requires that

$$\rho_1 A_1 v_1 = \rho_2 A_2 v_2 \tag{20}$$

and

$$\rho_1 A_2 v_2 + \rho_e A_e v_e = \rho_3 (A_2 + A_e) v_3 = \rho_3 A_4 v_4 \tag{21}$$

if v_3 is the uniform velocity of the mixed stream at the end of the mixing section. The momentum equation for the flow through the mixing section is

$$(p_2 - p_3)(A_2 + A_3) = \rho_3 (A_2 + A_e) v_3^2 - \rho_1 A_2 v_2^2 - \rho_e A_e v_e^2 \tag{22}$$

if p_3 denotes the pressure of the mixed fluid at the velocity v_3. Finally, there is the thrust equation

$$T = \rho_3 A_4 v_4^2 - \rho_1 A_1 v_1^2 \tag{23}$$

Through these seven equations, it is possible to express seven of the variables in terms of the others. If the dependent variables are taken as p_2, v_2, p_3, v_3, A_4, v_4 and T, the solution leads through the relations

$$v_4 = \frac{\rho_e A_e v_e + \rho_1 A_1 v_1}{\rho_3 A_4} \tag{24}$$

and

$$A_4 = \frac{\rho_e A_e v_e + \rho_1 A_1 v_1}{\rho_3 \sqrt{\frac{\rho_1 v_1^2}{\rho_3}\left[1 - \left(\frac{A_1}{A_2}\right)^2\right] - \frac{1}{\rho_3^2}\left[\frac{\rho_e A_e v_e + \rho_1 A_1 v_1}{A_2 + A_e}\right]^2 + \frac{2\rho_e A_e v_e^2}{\rho_3(A_2 + A_e)} + \frac{2\rho_1 A_1^2 v_1^2}{\rho_3 A_2(A_2 + A_e)}}} \tag{25}$$

to

$$T = \rho_1 A_1 v_1^2 \left(\left[\frac{\rho_e A_e v_e}{\rho_1 A_1 v_1} + 1\right] \sqrt{\frac{\rho_1}{\rho_3}\left[1 - \left(\frac{A_1}{A_2}\right)^2\right] - \frac{1}{\rho_3^2 v_1^2}\left[\frac{\rho_e A_e v_e + \rho_1 A_1 v_1}{A_2 + A_e}\right]^2 + \frac{2\rho_e A_e v_e^2}{\rho_3(A_2 + A_3)v_1^2} + \frac{2\rho_1 A_1^2}{\rho_3 A_2(A_2 + A_3)}} - 1 \right) \tag{26}$$

The complexity of this expression makes it difficult to recognize the influences of the different basic variables on the thrust. Some idea of those influences may, however, be gained by assigning reasonable values to some of the quantities, and finding how the thrust varies with the remaining one or two quantities. For example, a jet of constant mass flow and speed may be assumed. This fixes the thrust that would be given by the jet if released in free air. Assuming, next, that the exhaust gas is to mix with air in a constant proportion, the entrance area A_1, the basic stream velocity v_1 and the basic stream density ρ_1 may be assigned fixed values. This leaves to be varied the density ρ_e of the exhaust gas, and the area $A_2 + A_e$ of the parallel-sided portion of the duct.

Fig. 4 shows the result of this procedure for A_1 = 1 sq.ft., v_1 = 200 ft./sec., ρ_1 = 0.00239 slugs/cu.ft., and an exhaust mass flow $\rho_e A_e v_e$ = 0.03 slugs/sec., which corresponds to the air capacity of a 500 hp. engine. The exhaust velocity is taken as 600 ft./sec., about what would be used in practice. The exhaust

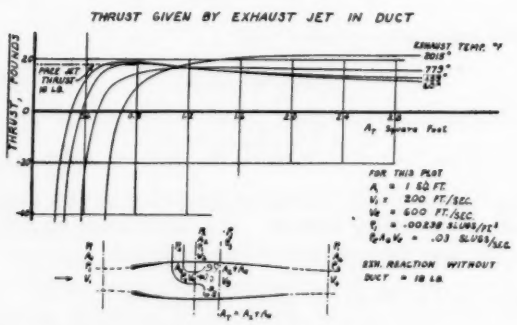
THRUST GIVEN BY EXHAUST JET IN DUCT
THRUST, POUNDS
FREE JET THRUST = 18 LB.
EXHAUST TEMP. °F
2015°
779°
A_T Square Feet
FOR THIS PLOT
A_1 = 1 SQ. FT.
V_1 = 200 FT./SEC.
V_e = 600 FT./SEC.
ρ_1 = .00238 SLUGS/FT³
$\rho_e A_e V_e$ = .03 SLUGS/SEC.
ESTIMATED REACTION WITHOUT DUCT = 18 LB.

FIG. 4. Effect of ducting on thrust of exhaust jet.

flow would then require a pipe 1.96 inches in diameter if the flow consisted of cold air, or 4.2 inches for exhaust gas at 2000°F.—the properties of the exhaust gas being taken as those of air, since both the gas and the air contain mostly nitrogen.

Under the conditions assumed, the exhaust thrust in free air would be 18 lbs. If the exhaust were at room temperature, a duct with a throat area about 0.7 times the inlet area would give the maximum improvement, but even so would only raise the thrust about 5 per cent. As the throat area of the duct is made less than the entrance area, the thrust becomes less than that of the free jet. To secure a thrust augmentor effect, it is thus necessary to speed up the duct air so that it will mix with the exhaust without too much kinetic loss. If this speeding up is carried too far, however, the net throat area becomes so small that a very large exit area is necessary to suck through the desired amount of duct air. This slows down the emerging stream, and results in a diminished, or even negative, thrust.

From the other curves in Fig. 4, it is seen that mild warming of the exhaust reduces the attainable thrust augmentation, but that an increased augmentation again is possible with a very hot exhaust. The augmentation in the latter case requires a duct with a throat area larger than the inlet area. This means that the augmentor action has become predominantly the result of a utilization of the exhaust heat, analogous to the utilization of the heat furnished by a ducted radiator. As in the case of the radiator, a large amount of heat is needed for any appreciable effect. Thus, a maximum thrust of 22 lbs., or an augmentation of but 4 lbs., could be obtained if the temperature of the exhaust gas were 2000°F., *i.e.*, about 300°F. above the normal temperature of such gases.

These observations suggest that it is impossible to utilize for thrust augmentation both the kinetic and the thermal energy of the exhaust. In a venturi-shaped duct, which serves to extract kinetic energy, there is a loss for thermodynamic reasons. A duct of the expanding-contracting type gives beneficial results on the thermodynamic side, but produces increased kinetic losses; and though the extra heating brought about by the losses in the latter case may be indirectly helpful, it has very little effect because of the low efficiency of the thermodynamic process. Any marked thrust augmentation presupposes, then, a large disparity between the thermal and kinetic energies extractable from the exhaust, with a consequent possibility of drawing on one of these energies without serious losses on account of the other.

The full possibilities of thrust augmentation are, of course, not indicated by Fig. 4, which merely represents one special case. Better results could certainly be found at higher velocities v_1, where the propulsive effect of the heating would be more pronounced. As the heat energy in the exhaust jet is about four times as great as the heat energy passing through the radiator, the exhaust thrust might be raised to something like four times the radiator thrust by proper ducting. This would represent a substantial augmentation under favorable conditions. If the radiator is already ducted, a simple way of utilizing the exhaust would then be to discharge it in the radiator duct just behind the radiator. In an air-cooled installation, this would be accomplished by releasing the exhaust inside the cowling without other manifolding.

Results Based on Exit Area of Duct

The area A_1, on which the thrust has been based in the analysis so far, must itself be determined through a supplementary calculation. To this end, it is convenient to put Eq. (25) into the form

$$\left[\rho_1 A_1 v_1\right]^2\left\{\left[1-\frac{2A_2}{A_2+A_e}\right]+\frac{\rho_1}{\rho_3}\left[\frac{A_2^2}{A_4^2}+\frac{A_2^2}{(A_2+A_e)^2}\right]\right\}$$
$$+2\left[\rho_1 A_1 v_1\right]\left[\rho_e A_e v_e\right]\left\{\frac{\rho_1}{\rho_3}\left[\frac{A_2^2}{A_4^2}+\frac{A_2^2}{(A_2+A_e)^2}\right]\right\}+$$
$$\left[\rho_e A_e v_e\right]^2\left\{\frac{\rho_1}{\rho_3}\left[\frac{A_2^2}{A_4^2}+\frac{A_2^2}{(A_2+A_e)^2}\right]-\left[\frac{\rho_1 A_2 v_1}{\rho_e A_e v_e}\right]^2-\right.$$
$$\left.2\frac{\rho_1}{\rho_e}\left[\frac{A_2^2}{A_e(A_2+A_e)}\right]\right\}=0 \quad (27)$$

and to introduce the abbreviations

$$\lambda=\frac{2A_2}{A_2+A_e}-1$$

$$\mu=\frac{\rho_1}{\rho_3}\left[\frac{A_2^2}{A_4^2}+\frac{A_2^2}{(A_2+A_e)^2}\right]$$

$$\nu=\left[\frac{\rho_1 A_2 v_1}{\rho_e A_e v_e}\right]^2+2\frac{\rho_1}{\rho_e}\left[\frac{A_2^2}{A_e(A_2+A_e)}\right]$$

through which the equation is reduced to

$$(\mu-\lambda)(\rho_1 A_1 v_1)^2+2\mu(\rho_1 A_1 v_1)(\rho_e A_e v_e)+(\mu-\nu)(\rho_e A_e v_e)^2=0 \quad (28)$$

Then,

$$\rho_1 A_1 v_1=\rho_e A_e v_e\left\{\frac{-\mu+\sqrt{\mu^2-(\mu-\lambda)(\mu-\nu)}}{\mu-\lambda}\right\} \quad (29)$$

and, by Eqs. (23) and (24),

$$T=\frac{\rho_e^2 A_e^2 v_e^2}{\rho_3 A_4}\left[1+\frac{\rho_1 A_1 v_1}{\rho_e A_e v_e}\right]^2-\rho_1 A_1 v_1^2$$
$$=T_e\left\{\frac{\rho_e A_e}{\rho_3 A_4}\left[\frac{-\lambda+\sqrt{\mu^2+(\mu-\lambda)(\nu-\mu)}}{\mu-\lambda}\right]^2-\right.$$
$$\left.\frac{v_1}{v_e}\left[\frac{-\mu+\sqrt{\mu^2+(\mu-\lambda)(\nu-\mu)}}{\mu-\lambda}\right]\right\} \quad (30)$$

with $T_e=\rho_e A_e v_e^2$ the thrust that would be furnished by the exhaust jet if there were no duct. The quantity in curved brackets might thus be termed the *augmentation factor* for the ducted arrangement.

Instead of the area A_1 used before, the thrust expression now contains the area A_4. By the logic already followed in the case of the ducted radiator, A_4 may be assumed to equal the exit area of the duct if the expansion or contraction of the duct toward that area is reasonably gradual. This leaves the thrust completely defined by quantities known directly in any given case.

Aside from making the solution of the problem more definite, the use of A_4 instead of A_1 has the advantage of removing the difficulty of handling the case of $v_1 = 0$, for which the thrust expression in terms of A_1, with $A_1 = \infty$, would become indeterminate, while the formula based on A_4 gives at once

$$T=T_e\frac{\rho_e A_e}{\rho_3 A_4}\left[\frac{-\lambda+\sqrt{\mu^2+(\mu-\lambda)(\nu-\mu)}}{(\mu-\lambda)}\right]^2 \quad (31)$$

Experimental Sidelights on Augmentor Theory

In a few rough preliminary tests on ducted jets, the results have been found to agree closely with those predicted by the foregoing theory.[9] Earlier findings by Schubauer[10] suggest that the cool jet augmentation shown in Fig. 4 for a particular case is typical of the thrust increases that may be secured without heating. The more pronounced augmentor effects found by Jacobs and Shoemaker[11] are also in line with the theory. For, since the driving jet in the experiments of these authors came from a high pressure tank at nearly atmospheric temperature, the jet was presumably much colder than the augmentor air. In the case of a duct of the venturi type, such as was used, cooling produces the same sort of propulsive effects as heating does in the case of an expanding-contracting duct. The direct augmentor ability of the duct was therefore supplemented by helpful thermodynamic effects, and a substantial total augmentation seems not unreasonable.

Exhaust Collectors vs. Individual Stacks

The foregoing analysis presumes steady flow conditions and applies therefore only to exhaust streams fed by numerous cylinders. Such collected streams are generally much slower than the free blasts from cylinders with individual stacks. This means that exhaust collection reduces the net impulse $\int F dt$ on the discharged gases, and hence the work $\int F ds = \int F v_1 dt = v_1 \int F dt$ done by the net exhaust reaction F on the engine moving at the velocity v_1. If the noise and glare of unmuffled exhaust flashes could be tolerated, or could be blanketed from view and hearing, it would thus be advantageous to use individual stacks, preferably shaped into expanding nozzles. There is some indication[8] that augmentor effects can be secured with intermittent jets as well as with continuous ones. It seems, however, hopeless to attempt a treatment of these effects along the elementary lines of this paper.

REFERENCES

[1] Meredith, F. W., *Cooling of Aircraft Engines*, British R. & M. No. 1683, August, 1935.

[2] Weise, A., *The Conversion of Energy in a Radiator*, N.A.C.A. Technical Memorandum No. 869 (Translated from *Vorträge der Hauptversammlung der Lilienthal Gesellschaft*, München, 1937, pages 269–276).

[3] Winter, H., *Contribution to the Theory of the Heated Ducted Radiator*, N.A.C.A. Technical Memorandum No. 893 (Translated from *Luftfahrtforschung*, Vol. 15, Nos. 10–11, October 10, 1938).

[4] Göthert, B., *The Drag of Airplane Radiators*, N.A.C.A. Technical Memorandum No. 896 (Translated from *Luftfahrtforschung*, Vol. 15, No. 9, September 10, 1938).

[5] Kimmel, H., *Theorie der Luftschrauben auf Aerodynamischer Grundlage*, R. Oldenbourg, Münich, 1912.

[6] Rauscher, M., *Some Secondary Factors Affecting Aircraft Performance*, Journal of the Aeronautical Sciences, Vol. 3, No. 10, August, 1936, pages 368–369.

[7] Buckingham, E., *Jet Propulsion for Airplanes*, N.A.C.A. Technical Report No. 159, 1923.

[8] Melot, H. F., *On Jet Propulsion*. (Quoted in *Scientific American*, April, 1926, pages 266–268).

[9] Phillips, W. H., *Jet Propulsion*, Master's Thesis, Massachusetts Institute of Technology, 1940.

[10] Schubauer, G. B., *Jet Propulsion*, N.A.C.A. Technical Note No. 442, January, 1933.

[11] Jacobs, E. N., and Shoemaker, J. M., *Tests on Thrust Augmentors for Jet Propulsion*, N.A.C.A. Technical Note No. 431, September, 1932.

Institute Notes

Honorary Fellow and Fellows Elected

The Fellows of the Institute have elected Dr. George W. Lewis an Honorary Fellow. Dr. Lewis is Director of Research of the National Advisory Committee for Aeronautics and a Past President of the Institute. He received the Daniel Guggenheim Medal in 1936 and delivered the Wilbur Wright Memorial Lecture before the Royal Aeronautical Society of Great Britain in 1939.

Ten American members of the Institute were elected as provided in the By-Laws to the grade of Fellow in 1940. The new Fellows are:

Allan Chilton, Project Engineer, Wright Aeronautical Corp.

Charles H. Colvin, Acting Chief, Instruments Div., U.S. Weather Bureau.

Smith J. De France, Engineer in Charge, Ames Aeronautical Laboratory, N.A.C.A.

Melvin N. Gough, Senior Airplane Test Pilot, Langley Memorial Aeronautical Laboratory, N.A.C.A.

Sam D. Heron, Research Engineer, Ethyl Gasoline Corp.

Paul H. Kemmer, Materiel Div., U.S. Army Air Corps, Wright Field.

Paul Kollsman, Director & Vice-Pres., Square D Company, in charge Kollsman Instrument Div.

George A. Page, Jr., Chief Engineer, St. Louis Airplane Div., Curtiss-Wright Corp.

F. W. Reichelderfer, Chief, U.S. Weather Bureau.

Igor Alexis Sikorsky, Aero. Engineer, Vought-Sikorsky Aircraft, United Aircraft Corp.

Dr. Louis H. Bauer Receives John Jeffries Award for 1940

Louis H. Bauer, M.D., of Hempstead, N.Y., was named the first recipient of the John Jeffries Award recently established by the Institute, for his pioneering work and continuing activity in advancing the interests of aviation medicine through twenty-one years of teaching, research, organization, editing and contributions to the literature. In recognition of the importance to aviation of scientific endeavor in the field of medicine, the Institute presents the John Jeffries Award annually for outstanding contributions to the advancement of aeronautics through medical research.

Dr. Bauer was graduated from Harvard College and Medical School and entered the Medical Corps of the U.S. Army in 1913. He was the first commandant of the School of Aviation Medicine of the Army Air Corps which he organized at Mitchel Field in 1919. He was the first Medical Director of the Aeronautics Branch of the Department of Commerce. Dr. Bauer organized and was the first president of the Aero Medical Association and is now editor-in-chief of its official publication, the Journal of Aviation Medicine. He is chief cardiologist at Meadowbrook Hospital, Hempstead, N.Y., a member of the staffs of other Long Island hospitals, and consultant in aviation medicine and cardiology to the Civil Aeronautics Administration. He is a Fellow of the American College of Physicians.

Henry G. Houghton Named for Robert M. Losey Award for 1940

Henry G. Houghton, Jr., Assistant Professor of Meteorology at Massachusetts Institute of Technology, was chosen by the Committee of Award to receive the 1940 Robert M. Losey Award for outstanding contributions to the science of meteorology as applied to aeronautics, presented for the first time at the Honors Night Dinner on January 28th. He receives the award for fundamental research in physical meteorology on the processes of condensation in the atmosphere.

Mr. Houghton was born in New York City in 1905. He brings to the field of meteorology the training and research methods of a physicist and electrical engineer, having studied at Drexel Institute of Technology and received the degree of S.M. in Electrical Engineering from Massachusetts Institute of Technology in 1927. Following graduation, his meteorological work at the Round Hill Research Station and Massachusetts Institute of Technology dealt with the fundamental physical properties of atmospheric fog, apparatus and methods for measuring fog particles and the resistance of fog and clouds to the transmission of visible light and radiant rays. This led to his development, with the assistance of W. H. Radford in 1938, of a means for clearing up fog over local areas by the use of a calcium chloride spray. This method, described by Dr. Sverre Petterssen in his recent Wright Brothers Lecture, is one of the first practically tested ways for artificially dissipating fog, although its application is limited.

Mr. Houghton's recent research has been an extension of similar studies in atmospheric condensation processes; i.e., the formation of fog, clouds, water droplets and ice particles in clouds and icing on aircraft in flight. His work on the underlying principles of these phenomena and precise measurement of their characteristics have contributed substantially to greater exactness in the science of weather forecasting and increased safety in air travel. He is a Fellow of the American Association for the Advancement of Science and a member of the American Physical Society, the American Meteorological Society, Sigma Xi and Tau Beta Pi.

Report on Ninth Annual Meeting to be in March Issue of Journal

Since this issue of the Journal went to press before the Honors Night Dinner and the Ninth Annual Meeting of the Institute, January 28th to 31st, complete accounts of the Dinner and Meeting will be published in the March issue.

Personnel Opportunities

The Personnel Bureau serves individual members, as well as organizations seeking to employ aeronautical specialists. Any member or organization may have requirements listed without charge.

Wanted

Small California aircraft manufacturing company with a plywood plastic project needs several senior layout men with stress analysis experience; also a project engineer. Please include complete information regarding experience and salary. Address reply to Box 121, Institute of the Aeronautical Sciences.

Aircraft Accessories Sales Engineers. Positions open to young men of proven ability in this field or allied fields. No applications considered without complete historical background and proof of ability. Must be willing to travel and locate anywhere in U.S. Address reply to Box 122, Institute of the Aeronautical Sciences.

Aircraft Accessories Design or Project Engineers. Positions open to young men of proven ability in this field or allied fields. No applications considered without complete historical background and proof of ability. Location Cleveland. Address reply to Box 123, Institute of the Aeronautical Sciences.

Available

Executive, associated with aircraft industry for 24 years. B.S.E. (Ae.E.) and Ae.E. degrees. Aero. Engineer, U.S. Army and U.S. Navy. Consulting Engineer, Project Engineer and Chief Engineer. Address reply to Box 124, Institute of the Aeronautical Sciences.

Student Branches

University of California. Mr. A. F. Bonnalie, of United Air Lines Transport Corporation, gave a talk on "Economic Highlights in Air Transportation" at a meeting held on October 3rd. A motion picture describing the Langley Memorial Aeronautical Laboratory of the N.A.C.A. was shown and discussed by Mr. Carlton Bioletti at a meeting held on November 7th.

Carnegie Institute of Technology. The Fourth Wright Brothers Lecture by Dr. Sverre Petterssen on "Recent Fog Investigations" was delivered by Walter E. Mortlock at a meeting held on December 19th. D. M. O'Keefe, Chief Meteorologist, of Pennsylvania-Central Airlines, and his assistant, O. P. Braun, participated in a discussion which followed.

Oregon State College. At a meeting held on December 11th, R. E. Herr, of the General Inspection Division of the C.A.A., spoke on the engineering aspects of his work.

Rensselaer Polytechnic Institute. On December 5th, Dr. Paul Hemke, Head of the Aeronautical Engineering Department, gave a talk on "High Speed Visual Flow Research."

The Technical Information Service
of the
Institute of the Aeronautical Sciences

This service has experienced personnel under the supervision of trained aeronautical engineers to compile any information desired. The services range from listing specialized reference books to the preparation of exhaustive bibliographies, digesting of reports and general surveys of any aeronautical subject.

Some of the available services are:

Bibliographies on any aeronautical subject.

Reports on any aeronautical subject.

Digests of aeronautical books, papers, periodicals and references.

Translations in all languages.

Engineering investigations of special aeronautical subjects.

Biographies of individuals engaged in aeronautics.

Photostats of any aeronautical or general engineering material.

Microfilms made on special order.

Photographs made from the Institute's photographic collection.

Drawings and tracings made.

In addition to the services mentioned any commission which comes within the scope of the Service will be accepted.

Research work is charged at the usual library fee of $2.00 per hour. Special arrangements may be made for work requiring several weeks or months.

Translators are available for accurate transcriptions of all foreign language data. Translations are carefully edited by trained engineers at the standard rate of 1¢ per word. Minimum charge, $2.00.

Reproductions of any material in the Aeronautical Archives of the Institute may be ordered at standard photostat rates.

SUGGESTIONS FOR CONTRIBUTORS TO THE JOURNAL *of the* AERONAUTICAL SCIENCES

The Institute of the Aeronautical Sciences invites both members and non-members from any country to submit papers for publication in the Journal of the Aeronautical Sciences. The Journal, following the practice of other scientific publications, does not pay for contributions.

The following directions for the preparation of papers, if followed by authors, will save correspondence, avoid the return of papers for changes, minimize the work of preparation for the printer, and save the expense due to the charges made for "author's corrections."

MANUSCRIPTS: Papers must be written in English, in original typewriting on one side only of white paper sheets, consecutively numbered, and be double or triple spaced with wide margins. Manuscripts should be prepared with great care so that they will be typographically accurate. Paragraphing should be given special attention. Papers should be written in the third person, reference to the writer being made as "the author." Avoid the use of the words "I," "we," and "you." Blueprint copies of papers are unacceptable as it is impossible to mark directions to the printer on them. Correcting, changing, or adding to papers after they are in type is costly. It is, therefore, imperative that papers submitted be in final form. Typographical errors may be corrected on proofs, but if authors wish to add material, they may do so at their own expense. In mailing, drawings may be rolled, but manuscripts should be sent flat. Send by first class mail (register if you wish for your own protection) to the Secretary, Institute of the Aeronautical Sciences, 1505 RCA Bldg. West, Rockefeller Center, New York City. All manuscripts will be examined by the Editorial Committee and by the Editor. Authors will be advised as promptly as possible (usually two to three weeks) whether the paper is acceptable for publication.

TITLES: The title of the paper should be brief. The name and initials of the author should be written as he prefers. The use of the full name of an author is advocated because of the frequent duplication of initials and surnames which sometimes makes it difficult to establish the identity of the author. This is particularly important for large annual indexing and abstracting services. All titles and degrees or honors are omitted. The name of the organization with which the author is associated should be placed after his name on the same line. The date on which the paper is received will be inserted by the Editor.

SUMMARIES OR ABSTRACTS: An abstract to be printed at the beginning should accompany each article. It should be adequate as an *index* and as a *summary*. It should contain a statement of major conclusions reached, since summaries in many cases constitute the only source of information used in compiling scientific reference indexes. Abstracts printed in other journals, especially foreign, in most cases, consist of summaries from printed papers. The summary should explain as adequately as possible the major conclusions to a non-specialist in the subject. The summary should contain from 100 to 300 words, depending on the length of the paper.

SUB-HEADINGS: Sub-headings should be inserted by the author at frequent intervals. The work of editorial preparation will be simplified by the author providing many sub-headings. Owing to the breaking of columns and the insertion of illustrations, some of the sub-headings may have to be omitted.

SHORTENING OF PAPERS: Some papers, at the end, fill in only a portion of a page. This leaves much wasted blank space as succeeding articles are started at the top of a page. Authors should indicate by notation on the left-hand side of the page what matter may be omitted when "run overs" occur. This request is important as the Journal cannot afford in the future, as it has in its earlier issues, to have blank half pages or more at the end of papers.

MATTER USUALLY DELETED: Acknowledgments of assistance in preparation of paper, except by collaborators. Photographs or illustrations of little technical interest and not showing advances in general practice. Too detailed tabular matter (general results of such tables may be included in the text). Lengthy descriptions of materials or processes or of preliminary experiments or theories which preceded final results; salient features only are of interest.

REFERENCES AND FOOTNOTES: References should appear as footnotes only, numbered consecutively, grouped together at the end of the manuscript. The arrangement should be as follows: (for books)—[1] Durand, W. F., *Aerodynamic Theory*, Vol. 1, p. 23; Julius Springer, Berlin, 1934. (For magazines)—Englund, C. R., Crawford, A. B., and Mumford, W. W., *Some Results of a Study of Ultra-Short-Wave Transmission Phenomenon*, Proc. I. R. E., Vol. 20, No. 12, pp. 481 and 482, March, 1933. Please give Author, Title, Volume, page, publisher and date of publication as indicated. Omission of one required fact causes much extra editorial work and possible inaccuracies. All references are grouped at the end of the article.

ILLUSTRATIONS: Illustrations should accompany manuscripts and each should always be referred to in the text, preferably by number. Drawings or graphs should not be larger than 12×16 inches, and must be made with jet black India Ink on white paper or tracing cloth, the latter being preferred. *Do not use typewriter for lettering.* The smallest lettering on 8×10 inch figures should be no less than $^1/_4$ inch high. Cross-section paper (white with black lines) may be used, but should not have more than 4 lines per inch. If finer ruled paper is used, the major division lines should be drawn in with black ink, omitting the finer divisions. In the case of finely ruled paper, only blue-lined paper can be accepted. *Tracing paper and blueprints* are not acceptable. Lettering and all markings must be large enough to be readable after reduction. Mail rolled or flat, never fold. Drawings which cannot be reproduced (including pencil drawings) will be returned to the author for redrawing, thus delaying publication of the paper. Photographs should be very distinct and show clear black and white contrasts. They must be on glossy white paper. Avoid round and oval photographs.

CAPTIONS AND LEGENDS: Legends or captions must accompany each drawing or photograph submitted. If written on the drawing or photograph, they should be placed below and well outside the part to be reproduced. It is better to place them on separate sheets of paper pasted to the back of the drawings or photographs. Each table should have a caption such as Table 1, Table 2, Table 3, etc. Captions should be complete in themselves so as to make the data intelligible to the reader without reference to the text. A duplicate list of captions for figures should be included as the last page of the manuscript. Use "Fig. 1" (not Figure 1), Figs. 3 and 4, etc., in both the text and the numbering of illustrations. In the text, "Eq. (1)," or "Eqs. (1) and (2)" are preferable to "Equation (1)." In captions and legends, except for "Fig." and "Eq." and table headings, write all words in full; do not abbreviate. Avoid placing explanatory written matter in the drawings; it should be in the text.

MATHEMATICAL WORK: Only the very simplest formulae should be typewritten; all others should be very carefully written in pen and ink, the writing to be large enough so that ample room is provided to mark mathematical matter for the printer. A considerable space for marking should be allowed above and below all equations. All complicated equations should be repeated on separate sheets with plenty of space left for marking. The solidus should be used for simple fractions appearing within the text. Make all expressions clear to the typesetter. Greek letters used in formulae should be clearly designated by name on the margin of the manuscript. All symbols should be clearly written and carefully checked. The difference between capital and lower-case letters should be clearly distinguished and care taken to avoid confusion between zero (0) and the letter (o), between the numeral (one) and the letter (ell) and the prime ($'$), between alpha and a, kappa and k, u and mu, v and nu, n and eta. All subscripts and exponents should be clearly marked and dots and bars over letters or mathematical expressions should be avoided. Avoid complicated exponents and subscripts. When it is necessary to repeat a complicated expression, it should be represented by some convenient symbol.

NOMENCLATURE AND ABBREVIATIONS: The National Advisory Committee for Aeronautics Nomenclature should be used in preference to any others. Standard abbreviations should be used, and it should be noted that most abbreviations are lower case, such as m.p.h., b.m.e.p., i.hp., b.hp., hp., ... etc.